MANF is required for the postnatal expansion and maintenance of the pancreatic β-cell mass in mice

Tatiana Danilova[1], Ilya Belevich[1], Huini Li[1], Erik Palm[1], Eija Jokitalo[1], Timo Otonkoski[2,3] and Maria Lindahl[1]

[1]Institute of Biotechnology, HiLIFE, University of Helsinki, Finland.

[2] Research Programs Unit, Molecular Neurology, Biomedicum Stem Cell Center, University of Helsinki, Helsinki, Finland.

[3] Children's Hospital, Helsinki University Central Hospital, Helsinki, Finland.

Corresponding author:

Maria Lindahl, PhD

Institute of Biotechnology, PO Box 56 (Viikinkaari 5D), 00014 University of Helsinki, Finland,

phone +358405105455, email: maria.lindahl@helsinki.fi

ABSTRACT

Global lack of mesencephalic astrocyte-derived neurotropic factor (MANF) leads to progressive postnatal loss of β-cells mass and insulin-dependent diabetes in mice. Similarly to *Manf*$^{-/-}$ mice, embryonic ablation of MANF specifically from the pancreas results in diabetes. In this study, we assessed the importance of MANF for the postnatal expansion of the pancreatic β-cell mass and for adult β-cell maintenance in mice. Detailed analysis of *Pdx-1Cre*$^{+/-}$*::Manf*$^{fl/fl}$ mice revealed mosaic MANF expression in postnatal pancreases and significant correlation between the number of MANF-positive β-cells and β-cell mass in individual mice. *In vitro,* recombinant MANF induced β-cell proliferation in islets from aged mice and protected from hyperglycemia-induced endoplasmic reticulum (ER) stress. Consequently, excision of MANF from β-cells of adult *MIP-1Cre*^{ERT}*::Manf*$^{fl/fl}$ mice resulted in reduced β-cell mass and diabetes caused largely by β-cell ER

Diabetes Publish Ahead of Print, published online October 10, 2018

stress and apoptosis, possibly accompanied by β-cell de-differentiation and reduced rates of β-cell proliferation. Thus, MANF expression in adult mouse β-cells is needed for their maintenance *in vivo.* We also revealed a mechanistic link between ER stress, and inflammatory signaling pathways leading to β-cell death in the absence of MANF. Hence, MANF might be a potential target for regenerative therapy in diabetes.

INTRODUCTION

Insulin deficiency caused by autoimmune destruction of β-cells leads to type 1 diabetes (T1D) and β-cell death is also involved in the failure of insulin secretion that leads to type 2 diabetes (T2D) (1,2). Current diabetes therapies are based on treating hyperglycaemia, but they are not targeting basic disease mechanisms. As the prevalence of diabetes is rapidly increasing worldwide, it is important to develop new therapies to protect and restore the functional β-cell mass (3).

Increasing evidence suggests that ER stress followed by prolonged activation of the UPR is one of the pathogenic mechanisms leading to β-cell death in both T1D and T2D (4-6). Pancreatic β-cells are especially vulnerable to ER stress-mediated cell death due to their heavy demand of insulin production, depending of proper folding and secretion (7). ER stress is triggered by the accumulation of unfolded and misfolded proteins in the ER lumen leading to activation of UPR signalling cascades, which are mediated by three ER transmembrane protein sensors - PKR-like ER kinase (PERK), activating transcription factor 6 (ATF6) and inositol-requiring enzyme 1 (IRE1) (8). Mutations inactivating the *PERK* gene leads to ER dysfunction, neonatal diabetes and growth defects in patients with Wolcott-Rallison syndrome (WRS) (9). Similarly, a homozygous mutation in the *Perk* gene leads to retarded growth and neonatal diabetes in mouse (10,11). In addition, inactivating mutations in several UPR genes result in β-cell death and diabetes in mice (12,13).

MANF was originally described as a secreted trophic factor for dopamine neurons *in vitro* with protective roles for neurons and cardiomyocytes in rodent disease models (14-17). The protective

effect of MANF has been suggested to depend on its ability to dampen ER stress (15,16,18,19). The mechanisms whereby MANF acts and enters cells are not fully understood. It was suggested to bind with its C-terminal KDEL-motif (RTDL) to a KDEL-receptor at the cell surface and thereby enter the cell (20). Recently, MANF was shown to bind to lipid sulfatides on the cell surface followed by endocytosis (21). We recently discovered that MANF-deficiency in mice (*Manf*$^{-/-}$ mice) led to postnatal reduction of the pancreatic β-cell mass and severe insulin-deficient diabetes due to decreased β-cell proliferation and increased β-cell death (22). ER stress and chronic activation of the UPR in β-cells was found to precede the loss of β-cells in *Manf*$^{-/-}$ mice (22). Importantly, adeno-associated virus (AAV) vector mediated overexpression of MANF was able to regenerate β-cells *in vivo* and recombinant MANF was able to increase proliferation rates of β-cells *in vitro*, indicating that MANF protein is a potential new drug candidate for the treatment of T1D (22).

In the present study we examined the importance of MANF *in vivo* in mice by conditional removal of MANF specifically from pancreas and β-cells in embryo. Our results show that MANF expression in β-cells positively correlates with β-cell mass and negatively with β-cell apoptosis, further revealing the importance of MANF expression for β-cell survival. We further revealed the role of MANF for the adult β-cells by removal of MANF specifically from β-cells using *MIP-1Cre*^{ERT}*::Manf*$^{fl/fl}$ mice. This led to the development of diabetes caused by sustained ER stress resulting in increased β-cell death. Finally, we showed that MANF protein increased proliferation rates of even aged and MANF-deficient mouse β-cells *in vitro*. Thus, our work demonstrates that MANF is essential for the maintenance of adult β-cells in mice.

RESEARCH DESIGN AND METHODS

Animals and in vivo physiology

All experimental procedures involving mice were approved by the Finnish Animal Ethics Committee. All mice were kept on a 12 hour dark/light cycle with free access to chow diet and

water. The generation of *Manf*$^{-/-}$ and conditional *Manf*$^{fl/fl}$ mice has been described previously (22) and Supplementary text). To delete MANF embryonically from the pancreas we used a *Pdx-1Cre*^{TUV} transgenic mouse line (Jackson Laboratories, Stock 014647, C57BL/6J background) (23) crossed to *Manf*$^{fl/fl}$ mice (Hsd:ICR(CD-1) background). To specifically remove MANF from the β-cells in adult mice we used tamoxifen (TMX)-inducible *MIP1-CreERT*^{1Lphi} mice (24) (C57BL/6J background) crossed to *Manf*$^{fl/fl}$ mice (Hsd:ICR(CD-1) background). Eight-week-old *MIP-1Cre*^{ERT}*::Manf*$^{fl/fl}$ and *Manf*$^{fl/fl}$ mice were injected with either 33 mg/kg of Tmx or corn oil for 5 consecutive days. Four weeks post injection mice were sacrificed, tissues and sera analysed. All experimental animals were in mixed background. Analysis of blood samples were performed as described previously and in Supplementary Data.

Histological Analysis

Immunohistochemistry, quantification of β-cell mass, analysis of β-cell death were performed as described previously (22). For immunohistochemistry mouse pancreatic paraffin sections were stained with primary antibodies (Supplementary Table 1). For immunofluorescence staining appropriate secondary antibodies conjugated with Alexa Fluor® 488 or 568 (1:400, Molecular Probes, Life Technologies, Eugene, Oregon, USA) and DAPI (Vectorshield, Vector laboratories, Burlingame, USA) were used to visualize the labels.

In Vitro β-cell Proliferation

In vitro β-cell proliferation experiments were performed as previously described and assessed by Click-iT™ EdU Alexa Fluor™647 Imaging Kit (C10340, Invitrogen™, Thermofisher Scientific, Waltham MA, USA) (22). Isolated islets form 1.3 year old or 4-5 week old *Manf*$^{-/-}$ female mice were stimulated with recombinant human placental lactogen (500 ng/ml; Affiland) or recombinant human MANF (100 ng/ml; Icosagen) for 5 consecutive days in RPMI1640 media containing 11mM

glucose supplemented with 10% Fetal Bovine Serum (FBS) and antibiotics. Edu (10nM) was added to the culture medium for last 3 days of stimulation.

To study cell signalling pathways, islets from *Manf*$^{-/-}$ and control *Manf*$^{+/+}$ mice were kept overnight in RPMI1640 supplemented with 10% FBS. Next day islets were starved in 0.5% bovine serum albumin (BSA) in RPMI medium for 3 hour and stimulated with 100 ng/ml rhMANF for 1 hour followed by islets homogenisation in 1x Laemmli buffer and western blotting analysis.

Serial block-face scanning electron microscopy (SB-EM)

Mice were perfused with 4% formaldehyde followed by cutting of pancreases in pieces. The pieces were post-fixed, stained and embedded based on a previously published protocol (25). The collected images were processed, aligned and analyzed using Microscopy Image Browser (26).

Additional Materials and Methods

The methods for western blotting, RNA analysis and methods concerning treatment of murine islets, serial block-face scanning electron microscopy analysis and subcellular localization analysis are provided in the Supplementary Data.

Statistical Analysis

All data are presented as mean ± SEM. Statistical significance was assessed via Student t-test between 2 groups or one-way ANOVA followed by the Tukey's test between 4 groups as mentioned in the figure texts using GraphPad Prism 6 software (GraphPad Software, Inc., La Jolla,CA).

RESULTS

MANF is specifically expressed in β-cells in the islets of Langerhans

MANF is widely expressed in mouse tissues throughout the embryonic development and in adulthood (27). Detailed examination of MANF expression in the developing and adult mouse pancreas and islets revealed MANF expression in developing pancreatic primordium in E13.5 embryo by immunohistochemistry (IHC) (Fig. 1A), when major differentiation of pancreas-specific endocrine cells begins (28). Consistent with our previous studies, we observed wide expression of MANF in adult mouse pancreas with positive signal in both exocrine acinar cells and endocrine islets of Langerhans (Fig. 1B) (22,29,30). Importantly, no positive signal was detected in the pancreas of *Manf*$^{-/-}$ mice, confirming the specificity of MANF antibody used throughout this study (Fig. 1C-D, Supplementary Fig. 1.1D). QPCR and Western blotting analysis confirmed expression of *Manf* mRNA in pancreatic exocrine tissue and in isolated islets from adult mice (Fig. 1E-F). Thus, MANF protein is highly expressed in the mouse pancreas from early embryonic development until adulthood.

Next we studied MANF expression in detail in different islet endocrine cells by IHC. Although the majority of MANF-positive cells were insulin-positive β-cells (Fig. 1G-I), weak MANF expression was also observed in δ-cells (Fig. 1K-M), while almost no MANF signal was detected in α- (Fig. 1O-Q) or PP-cells (Fig. 1S-U). MANF was also co-expressed with cells expressing glucose transporter 2 (GLUT2) (Supplementary Fig. 1.1E-G) and pancreatic and duodenal homeobox 1 (PDX1) (Supplementary Fig. 1.1H-J), further confirming that MANF is predominantly expressed in insulin expressing β-cells of the islets.

Subcellular localization analysis revealed strong co-localization of MANF with the ER and insulin, a partial co-localization of MANF with GRP78 and a complete segregation of MANF from Golgi in the primary mouse islets cells based on the Mander's and Pearson correlation coefficients (Fig. 1W-Z, Supplementary Fig.1.1K-V, Supplementary Table 2).

Interestingly, in pancreas tissue from diabetic mice, we found increased MANF expression in some β-cells located near lymphocytic cells invading the islets of 12-week-old pre-diabetic NOD mice

(Supplementary Fig. 1.2A-L). Barely no MANF expression was detected in the lymphocytic cells characteristic for insulitis. In addition, increased expression of MANF was found in some β-cells of 8-week-old db/db mice (Supplementary Fig. 1.2M-Y).

MANF expression in β-cells is important for maintaining the β-cell mass in Pdx-1Cre$^{+/-}$::Manf$^{fl/fl}$ mice postnatally

Detailed characterization of the diabetic phenotype in *Pdx-1Cre*$^{+/-}$::*Manf*$^{fl/fl}$ mice revealed that embryonic deletion of MANF specifically from the pancreas resulted in the postnatal β-cell failure (Supplementary Fig. 2.1 and Supplementary Text) (22). However, the decreased β-cell mass and diabetic phenotype appeared in *Pdx-1Cre*$^{+/-}$::*Manf*$^{fl/fl}$ mice later than in the *Manf*$^{-/-}$ mice (Supplementary Fig. 2.1 and Supplementary Text) (22). No ectopic Cre activity affected MANF expression in the brain of *Pdx-1Cre*$^{+/-}$::*Manf*$^{fl/fl}$ mice as compared to *Manf*$^{fl/fl}$ mice (Supplementary Fig. 2.2A-J). Analysis of double transgenic *Pdx-1Cre*$^{+/-}$::*dtTomato* reporter mice revealed that Pdx-1Cre was not expressed in all MANF-expressing pancreatic cells during development or in adult islet endocrine and exocrine cells (Supplementary Fig. 2.2K-R and Supplementary Text). Consequently, we observed incomplete recombination in *Pdx-1Cre*$^{+/-}$::*Manf*$^{fl/fl}$ mice leading to mosaic expression of MANF both in exocrine tissue and endocrine islets in the postnatal and adult pancreas (Supplementary Fig. 2.3A-I, K). Strong mosaic MANF expression was detected in P14 and adult MANF conditional pancreases with individual degree of variation (Fig. 2F, Supplementary Fig. 2.3D-I). Some adult mice totally lacked MANF expression in the islets (Fig. 2C, Supplementary Fig. 2.3I). As expected, *Manf* mRNA levels in isolated islets from *Pdx-1Cre*$^{+/-}$::*Manf*$^{fl/fl}$ mice were significantly decreased at different postnatal stages, compared to *Manf*$^{fl/fl}$ islets and the expression of *Manf* mRNA in conditional islets increased with age (Supplementary Fig. 2.3J). Moreover, we observed loss of islet architecture and decreased intensity of insulin immunoreactivity in the pancreases lacking MANF (Fig. 2A-C, 2K, 2M, 2O), whereas islet

structure remained intact when MANF expression was present in most of the β-cells (Fig. 2D-F, 2J, 2L, 2N).

Furthermore, the number of double MANF- and insulin-positive cells correlated with the β-cell mass (Fig. 2P), and consequently with blood glucose levels in individual mice (Fig. 2Q). Quantification of TUNEL-positive insulin-positive β-cells revealed increased apoptosis in islets with increased number of β-cells lacking MANF (Fig. 2R).

MANF expression is required for maintaining β-cell phenotype in Pdx-1Cre$^{+/-}$::Manf$^{fl/fl}$ mice

Reduced β-cell mass in P14 and P56 conditional animals was accompanied with a significant reduction of β-cells markers *Glut2, insulin1/insulin2 (Ins1/2), Pdx1, MafA and glucokinase* (*Gck)* mRNA levels in islets of *Pdx-1Cre$^{+/-}$::Manf$^{fl/fl}$* mice (Fig. 3B-C, Supplementary Fig. 3A-C). This was expected since the proportion of β−cells compared to other islet cells, was decreased in the *Pdx-1Cre+/-::Manf$^{fl/fl}$* islets. No reduced expression levels of β-cell markers was observed in P1 islets (Fig. 3A) in contrast to what was observed in the conventional *Manf$^{-/-}$* islets (22). Moreover, GLUT2 and MANF double immunohistochemistry confirmed that absence of MANF in the β-cells was associated with loss of GLUT2 membrane localization (Fig. 3F-N).

UPR pathways are activated in isolated islets and pancreases from conventional *Manf$^{-/-}$* mice already before birth at E18.5 (20). Additionally, electron microscopy analysis of *Manf$^{-/-}$* β-cells revealed increased and expanded ER network with stacked and occasionally dilated sheets as a sign of ER stress in 4-week-old mice (Supplementary Fig. 3D-G, Supplementary Video1-2) (31-33).

Consistent with this, we observed significant upregulation of *Atf4, Grp78, Chop, spliced Xbp1 and total Xbp1*, but not *Atf6* mRNA levels in P1 conditional islets (Fig. 3D). At P14, we demonstrated continuous significant increase in mRNA levels of UPR markers (Fig. 3E). Altogether, activation of the main UPR sensors IRE-1, PERK and later ATF6 and their downstream targets seem to precede the loss of β-cell phenotype in *Pdx1-Cre$^{+/-}$::Manf$^{fl/fl}$* conditional islets.

Effects of recombinant MANF protein in vitro

We have previously demonstrated that recombinant human (rh)MANF protein stimulates proliferation of β-cells from young adult mice both *in vitro* and *in vivo* (22). Under normal conditions the primary mechanism for maintaining the postnatal β-cells mass is self-renewal of β-cells (34). Basal β-cell proliferation and response to mitogenic triggers declines markedly with age in both rodents and humans (35-37). To realistically model the effect of MANF on adult human β-cell dynamics we used islets from aged adult mice, where β-cell proliferation is extremely low. We found that rhMANF seem to increase β-cell proliferation rates *in vitro* even in islets isolated from aged, 15-month-old mice (Fig. 4A-J).

We previously demonstrated that MANF partially protects mouse β-cells from thapsigargin induced cell death *in vitro* (38). Herein, we analysed whether MANF protects isolated mouse islet β-cells from glucotoxicity. *Manf* mRNA levels were significantly upregulated in islets after exposure to hyperglycemia (Fig. 4K). In addition, we found increased expression of *spXbp1* mRNA in the islets treated with high glucose consistent with previous results (Fig. 4M) (39,40). Addition of rhMANF in the medium containing high glucose led to a significant decrease in the expression levels of *spXbp1* and *tXpb1* mRNA (Fig. 4L-N). Furthermore, MANF protein was able to induce proliferation of $Manf^{-/-}$ β-cells *in vitro* as well as significantly reduce the expression of UPR markers in isolated islets of $Manf^{-/-}$ mice (Supplementary Fig. 4A-C).

Deletion of MANF exclusively from adult pancreatic β-cells results in diabetes in MIP-1Cre^{ERT}::Manf$^{fl/fl}$ mice

To address whether MANF is required for adult β-cell survival and proliferation *in vivo* we specifically removed MANF from the β-cells in adult mice. TMX-injected *MIP-1Cre^{ERT}::Manf$^{fl/fl}$(TMX)* mice did not differ in weight, but random fed TMX-injected conditional mice had increased blood glucose levels and reduced serum insulin levels accompanied by impaired

glucose clearance, as compared to control mice after 4 weeks wash-out period of TMX injections (Fig. 5A-D, Supplementary Fig. 5.1A-B). Bolus injection of insulin normalized the blood glucose levels in *MIP-1Cre^{ERT}::Manf$^{fl/fl}$(TMX)* animals, suggesting intact insulin sensitivity (Supplementary Fig. 5.1C). The lower insulin levels after intraperitoneal glucose injection confirmed decreased insulin secretion in *MIP-1Cre^{ERT}::Manf$^{fl/fl}$(TMX)* animals (Supplementary Fig. 5.1D).

Basal and glucose stimulated insulin release from islets isolated from *MIP-1Cre^{ERT}::Manf$^{fl/fl}$(TMX)* mice was significantly lower compared to controls (Fig. 5E). Accordingly, islet insulin content was also reduced (Fig. 5F). However, as shown for *Manf$^{-/-}$* islets, their capacity to secrete insulin relative to cellular insulin content did not differ from controls and the response to IBMX was even increased (Fig. 5G).

Immunofluorescence staining revealed MANF expression in some β-cells four weeks after the TMX injection in *MIP-1Cre^{ERT}::Manf$^{fl/fl}$* mice (Fig. 5K-M). The relative proportion of double MANF-and insulin-positive β-cells observed in islets of TMX-injected mice was 15.22 ± 3.27% compared to islets of *MIP-1Cre^{ERT}::Manf$^{fl/fl}$(OIL)* controls suggesting incomplete recombination with a degree of β-cell regeneration during the 4-week wash-out period following tamoxifen-injections. We also observed some loss of MANF expression (14.8 ± 3.6%) in the insulin-positive β-cells of *MIP-1Cre^{ERT}::Manf$^{fl/fl}$(OIL)* islets (Fig. 5H-J, Supplementary Fig. 5.1F-W). This was in line with quantitative RT-PCR showing significantly reduced *Manf* mRNA levels in isolated islets from *MIP-1Cre^{ERT}::Manf$^{fl/fl}$(OIL)* mice compared to islets from oil-injected *Manf$^{fl/fl}$* and TMX-injected *Manf$^{fl/fl}$* mice suggesting some degree of leakiness resulting in Cre translocation to the nucleus even in the absence of TMX (Supplementary Fig. 5.1E). Compared to islets from *MIP-1Cre^{ERT}::Manf$^{fl/fl}$(OIL)* mice, *Manf* mRNA levels were significantly reduced in *MIP-1Cre^{ERT}::Manf$^{fl/fl}$(TMX)* islets (Supplementary Fig. 5.1E). Importantly, TMX seemed to repress *Manf* mRNA expression by itself in *Manf$^{fl/fl}$* islets (Supplementary Fig. 5.1E). MANF expression in

the brain did not differ between *MIP-1Cre^{ERT}::Manf$^{fl/fl}$(OIL)* and *MIP-1Cre^{ERT}::Manf$^{fl/fl}$(TMX)* mice (Supplementary Fig. 5.2A-J).

Immunoperoxidase staining of pancreatic sections 4 weeks after TMX-injection revealed that lack of MANF in the β-cells of adult *MIP-1Cre^{ERT}::Manf$^{fl/fl}$(TMX)* mice resulted in β-cell loss, decreased insulin expression and loss of islet architecture by redistribution of glucagon-stained α-cells into the core of islets (Fig. 5N-Q, Supplementary Fig. 5.1F-W). Significant reduction of the β-cell mass and islet cell mass, and a slight but non-significant increase in α-cell mass was observed in *MIP-1Cre^{ERT}::Manf$^{fl/fl}$(TMX)* pancreases compared to the control groups (Fig. 5R, Supplementary Fig. 5.1X-Z). Whereas the proliferation rate of insulin-positive β-cells in pancreases of *MIP-1Cre^{ERT}::Manf$^{fl/fl}$(OIL)* mice was 0.87 ± 0.08%, quantification of Ki67 positive insulin-positive β-cells revealed 50% reduction in proliferative β-cells in the *MIP-1Cre^{ERT}::Manf$^{fl/fl}$(TMX)* pancreases (0.45 ± 0.03%) (Fig. 5S). Additionally, the number of TUNEL positive insulin-positive β-cells were significantly increased in pancreases of *MIP-1Cre^{ERT}::Manf$^{fl/fl}$(TMX)* animals (4.4 ± 0.23%) compared to *MIP-1Cre^{ERT}::Manf$^{fl/fl}$(OIL)* (1.77 ± 0.11%) demonstrating increased β-cell apoptosis in pancreases of adult mutant mice (Fig. 5T).

Consistent with decreased β-cell mass in adult *Manf*-deleted mice, we found significant decrease in mRNA levels for *Glut2, Ins1/2, Pdx1* and *MafA,* but not *Gck,* in islets of *MIP-1Cre^{ERT}::Manf$^{fl/fl}$(TMX)* mice compared to control islets (Fig. 6A). In line with reduced expression of *Glut2* and *Pdx1* in islets we observed loss of GLUT2 membrane expression in β-cells where MANF was lacking (Fig. 6C-H). Reduced nuclear PDX1 staining was also detected in islets deficient for MANF at adult age (Fig. 6I-N). Thus, expression of MANF in β-cells is essential to maintain β-cell phenotype and mass also in adult mice.

MANF-deficiency in β-cells during development leads to increased and unresolved ER stress and chronic activation of the UPR response. In line with previous data, high levels of mRNA for *Grp78,*

Chop, Atf4, Atf6a and *Atf6β* were detected in islets from adult *MIP-1Cre^{ERT}::Manf$^{fl/fl}$(TMX)* mice (Fig. 6B). The level of *sXbp1* and *tXbp1* mRNA remained the same in both groups (Fig. 6B). Hence, increased and chronic activation of the UPR seem to be one of the mechanisms behind β-cell failure after MANF-deletion also in mature adult β-cells.

Insights in MANF mechanism of action

Differences in cell signalling pathways between wild-type (*Manf$^{+/+}$*) and MANF-deficient (*Manf$^{-/-}$*) islets were studied in the presence or absence of rhMANF *in vitro*. Previous studies have suggested that MANF exerts its protective effect on neurons through activation of the PI3K/AKT signalling pathways (41). We found a trend for increase in AKT (Ser473) phosphorylation in *Manf$^{+/+}$* islets after MANF addition (Fig. 7A, 7B), besides a detectable but non-significant upregulation of pan-AKT levels in MANF-treated islets (Supplementary Fig. 6C). A slight decrease in phospho-AKT was found in *Manf$^{-/-}$* islets, which was clearly though not significantly upregulated by addition of rhMANF (Fig. 7A, 7B, Supplementary Fig. 6C). Furthermore, Tribbles homolog 3 (*Trib3*) mRNA levels were significantly increased in MANF-deficient islets (Fig. 7C-D, Supplementary Fig. 6A). As *Trib3* mRNA expression is modulated by ATF4 in the PERK-UPR pathway and TRIB3 is a negative regulator of AKT, the reduced AKT phosphorylation in *Manf$^{-/-}$* islets might be caused by the chronic activation of ATF4 followed by increased TRIB3 expression (5,42,43). We also found a trend for slight decrease in the level of phospho-ERK1 (44 kDa) in *Manf$^{-/-}$* islets compared to *Manf$^{+/+}$* islets (Fig. 7E-F, Supplementary Fig. 6D). MANF has been shown to relieve NF-κB activation and downregulate BCL10 expression in human islets exposed to cytokines *in vitro* (30). As BCL10 is a known inducer of apoptosis and an upstream regulator of NF-κB signalling (44,45), we next tested whether NF-κB was differently regulated in β-cells *in vitro*. We found a trend for increased NF-κB phosphorylation in *Manf$^{-/-}$* islets compared to *Manf$^{+/+}$* islets (Fig. 7G-H, Supplementary Fig. 6E). Furthermore, BCL10, a binding partner of TRAF2 and a regulator of NF-

κB (46), was found significantly upregulated in *Pdx-1Cre*$^{+/-}$*::Manf*$^{fl/fl}$ islets at P1 (Fig. 7I,7J, Supplementary Fig. 6B). As IRE1α in prolonged ER stress forms a complex with apoptosis signal-regulating kinase-1 (ASK1) and TNF receptor-associated factor 2 (TRAF2) triggering JNK activation (47), we tested c-Jun activation in the *Manf*$^{-/-}$ islets. We observed a trend for increased phosphorylation of c-Jun (Ser63) in *Manf*$^{-/-}$ islets compared to *Manf*$^{+/+}$ controls (Fig 7K-L, Supplementary Fig. 6G). In addition to JNK, IRE1α stimulates the activation of p38MAPK that promotes apoptosis through phosphorylation of CHOP (48). A significant increase in levels of phospho-p38 was also detected in *Manf*$^{-/-}$ islets compared to controls (Fig. 7M-N, Supplementary Fig. 6F). In rat β-cells, NF-κB induces expression of inducible nitric oxide synthase (iNOS) and NO production (47). We found a trend for increased iNOS expression in the *Manf*$^{-/-}$ islets (Fig. 7O-P), thus suggesting NO production, inhibition of the SERCA-2b pump and depletion of $Ca2^{+}$ from the ER increasing the amplitude of ER stress (47).

DISCUSSION

We recently reported that global absence of MANF in mouse results in insulin deficient diabetes and reduced viability (22). Herein, we provide new insights for the role of MANF during pancreas development and in mature β-cells.

MANF expression in the developing and adult mouse was studied in detail revealing expression of MANF already in the endocrine pancreatic primordium during mouse embryonic development. Adult mouse pancreas exhibited MANF protein and *Manf* mRNA expression in both islets of Langerhans and pancreatic exocrine acinar cells. Importantly, in endocrine islets MANF was predominantly expressed in β-cells with some expression in δ-cells, but not in α- or PP-cells, comparable to results obtained in human islets (30). MANF protein levels are highly upregulated in pancreatic β-cells of $Ins2^{Akita}$ mice, where UPR is triggered by the accumulation of misfolded proinsulin in the ER leading to β-cell death (29,49,50). Here we provide evidence that MANF

expression was increased in β-cells near infiltrated lymphocytes in pre-diabetic NOD islets, in agreement with data showing increased *Manf* mRNA expression and UPR activation preceding the β–cell death in islets from pre-diabetic NOD mice (51,52). Increased MANF expression was detected in some β-cells in the islets of db/db mice, in line with recently published data (53). Conversely, MANF was downregulated as a consequence of reduced *Glis3* expression in β-cells diabetes-susceptible NOD mice, where chronic ER stress led to β-cell death (54). This study further support our results that MANF expression in β-cells is needed for restoring cellular homeostasis by preventing long term ER stress leading to β-cell apoptosis, senescence and diabetes.

Similarly to $Manf^{-/-}$ mice, $Pdx\text{-}1Cre^{+/-}$::$Manf^{fl/fl}$ mice developed hyperglycaemia and hypoinsulinemia due to postnatal reduced β-cell mass caused by reduced β-cell proliferation and increased β-cell death. However, due to mosaic Cre recombination some $Pdx\text{-}1Cre^{+/-}$::$Manf^{fl/fl}$ mice demonstrated patchy expression of MANF in both β-cells and exocrine acinar cells at P14 and onwards, suggesting clonal expansion of MANF-expressing cells in these pancreases. Importantly, ectopic Cre expression and recombination in the hypothalamic region of the brain of $Pdx\text{-}1Cre^{+/-}$ mice has been reported (55). However, MANF was not removed from hypothalamic neurons in the $Pdx\text{-}1Cre^{+/-}$::$Manf^{fl/fl}$ brain suggesting that the diabetic phenotype is solely caused by the pancreatic deletion of MANF.

We previously demonstrated that the β-cell mass is unaffected in E18.5 $Manf^{-/-}$ mice, but decreased by 50% in new born $Manf^{-/-}$ mice (22), suggesting that MANF is not needed for the development of β-cell mass before birth, but rather for the postnatal expansion of the β-cell mass. Here we demonstrated for the first time that the number of MANF-positive β-cells positively correlated with the β-cell mass as well as blood glucose levels and TUNEL-positive β-cells in individual $Pdx\text{-}1Cre^{+/-}$::$Manf^{fl/fl}$ mice. The delayed onset of diabetes in $Pdx\text{-}1Cre^{+/-}$::$Manf^{fl/fl}$ mice compared to conventional $Manf^{-/-}$ mice was likely due to an incomplete removal of MANF from the pancreas.

To directly address the role of MANF in mature β-cells, we specifically excised MANF from β-cells in adult mice. Although MANF was not completely deleted from all pancreatic β-cells in *MIP-1Cre^{ERT}::Manf$^{fl/fl}$(TMX)* mice, we demonstrated that lack of MANF in the adult β-cells resulted in reduced expression of β-cell specific genes, poor β-cell survival and proliferation leading to hyperglycemia and diabetes. The above results strongly argue against a systemic effect of circulating MANF in rescuing β-cells and clearly demonstrates that local expression of MANF is required to maintain the β-cell phenotype in mice (56,57). Furthermore, MANF expression in pancreatic exocrine acinar cells did not protect MANF-deficient adult β-cells.

The ability to stimulate adult β-cell proliferation and survival, inhibit β-cell apoptosis, and induce β-cell neogenesis would significantly progress the prospects of therapy for diabetes. Currently, a number of different factors and hormones have been identified that induce β-cell proliferation *in vitro* or/and *in vivo* (58,59). However, not many can enhance the rates of β-cell proliferation and restrain β-cell apoptosis at the same time. In this study, we demonstrated that MANF protein was able to intensify islet β-cell proliferation from aged mice, suggesting that MANF could partly reverse age-dependent repression of β-cell replication. Previously, we found that recombinant MANF protein partially rescued mouse and human β-cells from cytokine and ER stress-induced cell death in culture (30,38) and induced human β-cell proliferation (30). Here we showed that *Manf* mRNA was upregulated in mouse β-cells in hyperglycemic conditions *in vitro* and that MANF protein reduced ER stress-induced glucotoxicity in mouse β-cells. We showed that MANF protein induced β-cell proliferation and reduced ER stress in MANF-deficient islets. Previously we showed that inflammatory cytokines were able to increase MANF-secretion from human β-cells *in vitro* (30). These results strongly indicate that exogenous MANF acts in a paracrine manner by dampening ER stress thus favouring β-cell protection and proliferation.

It is still unknown how and where MANF exerts its beneficial effects. We show that it resides in the ER where it modulates ER stress and is crucial for β–cell survival. Upon ER stress, MANF is secreted from β–cells (30) and rhMANF have protective and restorative effects when applied exogenously to human and mouse β-cells (30,38). Thus MANF seems to have a dual mode of action 1) co-translationally inserted in the ER modulating ER stress and 2) extracellularly (possibly via autocrine/paracrine signaling) activating a signal transduction pathway or/and by being endocytosed and transported to the ER.

The identification of signaling receptors for MANF has been challenging. MANF with its suboptimal ER retention signal in its C-terminal domain, was found to weakly bind to KDEL receptor in the ER (20). The same study suggested that MANF also binds KDEL receptors at the cell membrane of cell-lines overexpressing KDELRs (20). However, direct binding of MANF to KDELR was not confirmed. Recently, MANF was reported to bind to lipid sulfatides (e.g. 3-O-sulfogalactosylceramide) located at the outer leaflet of cell membranes in *C. elegans* and in mammalian cells following MANF uptake by endocytosis into the cells (21). This report suggested that sulfatides are important for MANF cell surface binding, transport and secretion (21). The N-terminal domain of MANF contains a saposin-like domain known to be able to bind lipids (60). In addition, in the pancreas, sulfatides are selectively synthesized in β–cells but not in pancreatic exocrine tissue (61). Thus, exogenous MANF might be taken up by β–cells through lipid sulfatide binding and endocytosed back to ER where it relieves ER stress leading to restored proliferation and/or protection from ER stress-induced apoptosis. However, the increased mitogenic effect of MANF on β-cells might still depend on yet unidentified signaling receptor(s) and signaling cascades.

Previously we demonstrated the activation of all three UPR branches in pancreatic islets in *Manf*$^{-/-}$ mice (22). Herein we confirmed that chronic UPR activation and persistent ER stress in islets

lacking MANF is one of the mechanisms behind the reduced β-cell proliferation and increased β-cell death in islets from both *Pdx-1Cre*$^{+/-}$::*Manf*$^{fl/fl}$ mice and *MIP-1Cre*^{ERT}::*Manf*$^{fl/fl}$*(TMX)* mice. In addition, we showed a trend to decreased AKT phosphorylation and increased activation of inflammatory signalling in *Manf*$^{-/-}$ islets, probably caused by chronically activated UPR pathways. In agreement, we recently reported that MANF relieves cytokine-induced β-cell death through NF-κB inhibition in human β–cells (30). In addition, MANF was implicated as a negative regulator of inflammation by inhibiting expression of NF-κB target genes in the nucleus of fibroblast-like synoviocytes (62). Interestingly, platelet-derived growth factor (PDGF) released from injured retina promoted MANF expression in innate immune cells, and biased cells towards anti-inflammatory phenotype thereby promoting retinal tissue repair in mouse and fruitfly (63). Thus, roles for MANF in inflammation is emerging. In this study we have provided evidence for a mechanistic link between chronic ER stress and increased inflammation leading to β-cell death in *Manf*$^{-/-}$ islets (Fig. 7Q). A modest activation of the UPR has been suggested to adapt β-cells to the high demand of insulin production (10,64). Therefore, reduced insulin production by knockdown of insulin 2 gene in *Ins1*$^{-/-}$ background in adult mouse β-cells resulted in decreased PERK/eIF2α (65). The decrease in UPR led to an increase in proliferation through upregulation of the AKT/Cyclin D1 axis caused by a decrease in *Trib3* expression, suggesting that increased UPR signalling through peIF2α reduces β-cell proliferation. Similarly, addition of MANF to ER stressed β-cells might reduce ER stress and lead to increased β-cell proliferation. A recent study revealed that genetically-induced MANF overexpression in the hypothalamus led to increased feeding behavior and obesity in mice, caused by impaired insulin signaling and insulin-resistance in the hypothalamus (66). In contrast, decreased MANF-expression in the hypothalamus resulted in hypophagia and reduced body weight. Increased MANF at the ER was suggested to recruit and activate PIP4k2b, thus reducing AKT phosphorylation downstream of insulin receptor signaling leading to the hyperphagia (66). This result suggests that the cellular MANF levels are critical for insulin regulated AKT

phosphorylation. Thus, MANF-deficiency seems to result in ER stress, increased PERK/pEIF2α signaling, selective ATF4 translation inducing *Trib3* expression leading to reduced AKT phosphorylation and proliferation.

In conclusion, deletion of MANF from mouse β-cells both in early pancreatic development and in adulthood results in insulin-deficient diabetes. Consequently, endogenous MANF levels in β-cells correlates with β-cells survival in normal, diabetes-susceptible and stressed β-cells, but the precise mechanisms of MANF action needs further investigation. The ability of MANF to induce proliferation and at the same time protect β-cells from death makes it a promising drug candidate for the treatment of diabetes.

Author contributions

T.D. designed and performed experiments, and wrote the manuscript. I.B. and E.J. performed serial block-face scanning electron microscopy (SB-EM) experiments and analyzed the data. H.L. and E.P. performed experiments. T.O. designed experiments and revised the manuscript. M.L. designed and performed experiments, provided funding and wrote the manuscript. All authors accepted the final version of the manuscript.

Acknowledgements

S. Tynkkynen, Mari Heikkinen, Antti Salminen, and Mervi Lindman are thanked for excellent technical assistance. We acknowledge NIH KOMP for the MANF-targeted ESC clone used to develop the MANF knockout mice, FIMM High Content Imaging and Analysis unit services (University of Helsinki) for imaging and data analysis, Fluorescence or light microscopy images were captured with 3DHISTECH Panoramic 250 FLASH II digital slide scanner (Budapest, Hungary, with scanning service in the Institute of Biotechnology and in Research Programs Unit,

Faculty of Medicine, University of Helsinki, Biocenter Finland). This project was supported by the Juvenile Diabetes Research Foundation (JDRF) grant no. 17-2013-410, the Commission of the European Union, collaborative project MOLPARK, no. 400752, Sigrid Juselius Foundation, Academy of Finland Centre of Excellence grant, no.141122, Biocenter Finland (E.J, and I.B.) and Helsinki Institute of Life Science infrastructure. M.L. was supported by grants from the Finnish Diabetes Research Foundation and the Academy of Finland, grant no. 117044. Mart Saarma is acknowledged for financial support and for valuable comments on the manuscript. M.L. and T.D. are the guarantors of this work and, as such, had full access to all the data in the study and take responsibility for the integrity of the data and the accuracy of the data analysis. No potential conflicts of interest relevant to this article were reported.

References

1. Eizirik DL, Colli ML, Ortis F: The role of inflammation in insulitis and beta-cell loss in type 1 diabetes. Nat Rev Endocrinol 2009;5:219-226
2. Olokoba AB, Obateru OA, Olokoba LB: Type 2 diabetes mellitus: a review of current trends. Oman Med J 2012;27:269-273
3. Donath MY, Halban PA: Decreased beta-cell mass in diabetes: significance, mechanisms and therapeutic implications. Diabetologia 2004;47:581-589
4. Eizirik DL, Cnop M: ER stress in pancreatic beta cells: the thin red line between adaptation and failure. Sci Signal 2010;3:pe7
5. Eizirik DL, Miani M, Cardozo AK: Signalling danger: endoplasmic reticulum stress and the unfolded protein response in pancreatic islet inflammation. Diabetologia 2013;56:234-241
6. Cnop M, Foufelle F, Velloso LA: Endoplasmic reticulum stress, obesity and diabetes. Trends Mol Med 2012;18:59-68
7. Kaufman RJ, Back SH, Song B, Han J, Hassler J: The unfolded protein response is required to maintain the integrity of the endoplasmic reticulum, prevent oxidative stress and preserve differentiation in beta-cells. Diabetes Obes Metab 2010;12 Suppl 2:99-107
8. Ron D, Walter P: Signal integration in the endoplasmic reticulum unfolded protein response. Nat Rev Mol Cell Biol 2007;8:519-529
9. Delepine M, Nicolino M, Barrett T, Golamaully M, Lathrop GM, Julier C: EIF2AK3, encoding translation initiation factor 2-alpha kinase 3, is mutated in patients with Wolcott-Rallison syndrome. Nat Genet 2000;25:406-409
10. Harding HP, Ron D: Endoplasmic reticulum stress and the development of diabetes: a review. Diabetes 2002;51 Suppl 3:S455-461
11. Harding HP, Zeng H, Zhang Y, Jungries R, Chung P, Plesken H, Sabatini DD, Ron D: Diabetes mellitus and exocrine pancreatic dysfunction in perk-/- mice reveals a role for translational control in secretory cell survival. Mol Cell 2001;7:1153-1163
12. Hetz C: The unfolded protein response: controlling cell fate decisions under ER stress and beyond. Nat Rev Mol Cell Biol 2012;13:89-102
13. Scheuner D, Kaufman RJ: The unfolded protein response: a pathway that links insulin demand with beta-cell failure and diabetes. Endocr Rev 2008;29:317-333

14. Petrova P, Raibekas A, Pevsner J, Vigo N, Anafi M, Moore MK, Peaire AE, Shridhar V, Smith DI, Kelly J, Durocher Y, Commissiong JW: MANF: a new mesencephalic, astrocyte-derived neurotrophic factor with selectivity for dopaminergic neurons. J Mol Neurosci 2003;20:173-188
15. Glembotski CC, Thuerauf DJ, Huang C, Vekich JA, Gottlieb RA, Doroudgar S: Mesencephalic astrocyte-derived neurotrophic factor protects the heart from ischemic damage and is selectively secreted upon sarco/endoplasmic reticulum calcium depletion. J Biol Chem 2012;287:25893-25904
16. Airavaara M, Shen H, Kuo CC, Peranen J, Saarma M, Hoffer B, Wang Y: Mesencephalic astrocyte-derived neurotrophic factor reduces ischemic brain injury and promotes behavioral recovery in rats. J Comp Neurol 2009;515:116-124
17. Yang S, Huang S, Gaertig MA, Li XJ, Li S: Age-dependent decrease in chaperone activity impairs MANF expression, leading to Purkinje cell degeneration in inducible SCA17 mice. Neuron 2014;81:349-365
18. Apostolou A, Shen Y, Liang Y, Luo J, Fang S: Armet, a UPR-upregulated protein, inhibits cell proliferation and ER stress-induced cell death. Exp Cell Res 2008;314:2454-2467
19. Voutilainen MH, Back S, Porsti E, Toppinen L, Lindgren L, Lindholm P, Peranen J, Saarma M, Tuominen RK: Mesencephalic astrocyte-derived neurotrophic factor is neurorestorative in rat model of Parkinson's disease. J Neurosci 2009;29:9651-9659
20. Henderson MJ, Richie CT, Airavaara M, Wang Y, Harvey BK: Mesencephalic astrocyte-derived neurotrophic factor (MANF) secretion and cell surface binding are modulated by KDEL receptors. J Biol Chem 2013;288:4209-4225
21. Bai M, Vozdek R, Hnizda A, Jiang C, Wang B, Kuchar L, Li T, Zhang Y, Wood C, Feng L, Dang Y, Ma DK: Conserved roles of C. elegans and human MANFs in sulfatide binding and cytoprotection. Nat Commun 2018;9:897
22. Lindahl M, Danilova T, Palm E, Lindholm P, Voikar V, Hakonen E, Ustinov J, Andressoo JO, Harvey BK, Otonkoski T, Rossi J, Saarma M: MANF is indispensable for the proliferation and survival of pancreatic beta cells. Cell Rep 2014;7:366-375
23. Hingorani SR, Petricoin EF, Maitra A, Rajapakse V, King C, Jacobetz MA, Ross S, Conrads TP, Veenstra TD, Hitt BA, Kawaguchi Y, Johann D, Liotta LA, Crawford HC, Putt ME, Jacks T, Wright CV, Hruban RH, Lowy AM, Tuveson DA: Preinvasive and invasive ductal pancreatic cancer and its early detection in the mouse. Cancer Cell 2003;4:437-450
24. Tamarina NA, Roe MW, Philipson L: Characterization of mice expressing Ins1 gene promoter driven CreERT recombinase for conditional gene deletion in pancreatic beta-cells. Islets 2014;6:e27685
25. Deerinck TJ, Bushong E, Thor A. Ellisman MH. NCMIR methods for 3D EM: A new protocol for preparation of biological specimens for serial block-face SEM. Microscopy. 2010:6–8. https://ncmir.ucsd.edu/sbem-protocol
26. Belevich I, Joensuu M, Kumar D, Vihinen H, Jokitalo E: Microscopy Image Browser: A Platform for Segmentation and Analysis of Multidimensional Datasets. PLoS Biol 2016;14:e1002340
27. Lindholm P, Peranen J, Andressoo JO, Kalkkinen N, Kokaia Z, Lindvall O, Timmusk T, Saarma M: MANF is widely expressed in mammalian tissues and differently regulated after ischemic and epileptic insults in rodent brain. Mol Cell Neurosci 2008;39:356-371
28. Seymour PA, Sander M: Historical perspective: beginnings of the beta-cell: current perspectives in beta-cell development. Diabetes 2011;60:364-376
29. Mizobuchi N, Hoseki J, Kubota H, Toyokuni S, Nozaki J, Naitoh M, Koizumi A, Nagata K: ARMET is a soluble ER protein induced by the unfolded protein response via ERSE-II element. Cell Struct Funct 2007;32:41-50
30. Hakonen E, Chandra V, Fogarty CL, Yu NY, Ustinov J, Katayama S, Galli E, Danilova T, Lindholm P, Vartiainen A, Einarsdottir E, Krjutskov K, Kere J, Saarma M, Lindahl M, Otonkoski T: MANF protects human pancreatic beta cells against stress-induced cell death. Diabetologia 2018;
31. Akiyama M, Hatanaka M, Ohta Y, Ueda K, Yanai A, Uehara Y, Tanabe K, Tsuru M, Miyazaki M, Saeki S, Saito T, Shinoda K, Oka Y, Tanizawa Y: Increased insulin demand promotes while pioglitazone prevents pancreatic beta cell apoptosis in Wfs1 knockout mice. Diabetologia 2009;52:653-663

32. Riggs AC, Bernal-Mizrachi E, Ohsugi M, Wasson J, Fatrai S, Welling C, Murray J, Schmidt RE, Herrera PL, Permutt MA: Mice conditionally lacking the Wolfram gene in pancreatic islet beta cells exhibit diabetes as a result of enhanced endoplasmic reticulum stress and apoptosis. Diabetologia 2005;48:2313-2321
33. Wang J, Takeuchi T, Tanaka S, Kubo SK, Kayo T, Lu D, Takata K, Koizumi A, Izumi T: A mutation in the insulin 2 gene induces diabetes with severe pancreatic beta-cell dysfunction in the Mody mouse. J Clin Invest 1999;103:27-37
34. Dor Y, Brown J, Martinez OI, Melton DA: Adult pancreatic beta-cells are formed by self-duplication rather than stem-cell differentiation. Nature 2004;429:41-46
35. Teta M, Long SY, Wartschow LM, Rankin MM, Kushner JA: Very slow turnover of beta-cells in aged adult mice. Diabetes 2005;54:2557-2567
36. Kushner JA, Weir GC, Bonner-Weir S: Ductal origin hypothesis of pancreatic regeneration under attack. Cell Metab 2010;11:2-3
37. Kushner JA: The role of aging upon beta cell turnover. J Clin Invest 2013;123:990-995
38. Cunha DA, Cito M, Grieco FA, Cosentino C, Danilova T, Ladriere L, Lindahl M, Domanskyi A, Bugliani M, Marchetti P, Eizirik DL, Cnop M: Pancreatic beta-cell protection from inflammatory stress by the endoplasmic reticulum proteins thrombospondin 1 and mesencephalic astrocyte-derived neutrotrophic factor (MANF). J Biol Chem 2017;292:14977-14988
39. Elouil H, Bensellam M, Guiot Y, Vander Mierde D, Pascal SM, Schuit FC, Jonas JC: Acute nutrient regulation of the unfolded protein response and integrated stress response in cultured rat pancreatic islets. Diabetologia 2007;50:1442-1452
40. Lipson KL, Fonseca SG, Urano F: Endoplasmic reticulum stress-induced apoptosis and auto-immunity in diabetes. Curr Mol Med 2006;6:71-77
41. Zhang J, Tong W, Sun H, Jiang M, Shen Y, Liu Y, Gu H, Guo J, Fang J, Jin L: Nrf2-mediated neuroprotection by MANF against 6-OHDA-induced cell damage via PI3K/AKT/GSK3beta pathway. Exp Gerontol 2017;100:77-86
42. Cunard R: Mammalian tribbles homologs at the crossroads of endoplasmic reticulum stress and Mammalian target of rapamycin pathways. Scientifica (Cairo) 2013;2013:750871
43. Du K, Herzig S, Kulkarni RN, Montminy M: TRB3: a tribbles homolog that inhibits Akt/PKB activation by insulin in liver. Science 2003;300:1574-1577
44. Mazzone P, Scudiero I, Ferravante A, Paolucci M, D'Andrea LE, Varricchio E, Telesio G, De Maio C, Pizzulo M, Zotti T, Reale C, Vito P, Stilo R: Functional characterization of zebrafish (Danio rerio) Bcl10. PLoS One 2015;10:e0122365
45. Ruland J, Duncan GS, Elia A, del Barco Barrantes I, Nguyen L, Plyte S, Millar DG, Bouchard D, Wakeham A, Ohashi PS, Mak TW: Bcl10 is a positive regulator of antigen receptor-induced activation of NF-kappaB and neural tube closure. Cell 2001;104:33-42
46. Yoneda T, Imaizumi K, Maeda M, Yui D, Manabe T, Katayama T, Sato N, Gomi F, Morihara T, Mori Y, Miyoshi K, Hitomi J, Ugawa S, Yamada S, Okabe M, Tohyama M: Regulatory mechanisms of TRAF2-mediated signal transduction by Bcl10, a MALT lymphoma-associated protein. J Biol Chem 2000;275:11114-11120
47. Brozzi F, Eizirik DL: ER stress and the decline and fall of pancreatic beta cells in type 1 diabetes. Ups J Med Sci 2016;121:133-139
48. Ron D, Hubbard SR: How IRE1 reacts to ER stress. Cell 2008;132:24-26
49. Oyadomari S, Araki E, Mori M: Endoplasmic reticulum stress-mediated apoptosis in pancreatic beta-cells. Apoptosis 2002;7:335-345
50. Oyadomari S, Koizumi A, Takeda K, Gotoh T, Akira S, Araki E, Mori M: Targeted disruption of the Chop gene delays endoplasmic reticulum stress-mediated diabetes. J Clin Invest 2002;109:525-532
51. Morita S, Villalta SA, Feldman HC, Register AC, Rosenthal W, Hoffmann-Petersen IT, Mehdizadeh M, Ghosh R, Wang L, Colon-Negron K, Meza-Acevedo R, Backes BJ, Maly DJ, Bluestone JA, Papa FR: Targeting ABL-IRE1alpha Signaling Spares ER-Stressed Pancreatic beta Cells to Reverse Autoimmune Diabetes. Cell Metab 2017;25:883-897 e888
52. Tersey SA, Nishiki Y, Templin AT, Cabrera SM, Stull ND, Colvin SC, Evans-Molina C, Rickus JL, Maier B, Mirmira RG: Islet beta-cell endoplasmic reticulum stress precedes the onset of type 1 diabetes in the nonobese diabetic mouse model. Diabetes 2012;61:818-827

53. Neelankal John A, Ram R, Jiang FX: RNA-Seq Analysis of Islets to Characterise the Dedifferentiation in Type 2 Diabetes Model Mice db/db. Endocr Pathol 2018;
54. Sharma RB, O'Donnell AC, Stamateris RE, Ha B, McCloskey KM, Reynolds PR, Arvan P, Alonso LC: Insulin demand regulates beta cell number via the unfolded protein response. J Clin Invest 2015;125:3831-3846
55. Wicksteed B, Brissova M, Yan WB, Opland DM, Plank JL, Reinert RB, Dickson LM, Tamarina NA, Philipson LH, Shostak A, Bernal-Mizrachi E, Elghazi L, Roe MW, Labosky PA, Myers MG, Gannon M, Powers AC, Dempsey PJ: Conditional Gene Targeting in Mouse Pancreatic beta-Cells Analysis of Ectopic Cre Transgene Expression in the Brain. Diabetes 2010;59:3090-3098
56. Galli E, Harkonen T, Sainio MT, Ustav M, Toots U, Urtti A, Yliperttula M, Lindahl M, Knip M, Saarma M, Lindholm P: Increased circulating concentrations of mesencephalic astrocyte-derived neurotrophic factor in children with type 1 diabetes. Sci Rep 2016;6:29058
57. Wu T, Zhang F, Yang Q, Zhang Y, Liu Q, Jiang W, Cao H, Li D, Xie S, Tong N, He J: Circulating mesencephalic astrocyte-derived neurotrophic factor is increased in newly diagnosed prediabetic and diabetic patients, and is associated with insulin resistance. Endocr J 2017;64:403-410
58. Vasavada RC, Gonzalez-Pertusa JA, Fujinaka Y, Fiaschi-Taesch N, Cozar-Castellano I, Garcia-Ocana A: Growth factors and beta cell replication. Int J Biochem Cell Biol 2006;38:931-950
59. Tarabra E, Pelengaris S, Khan M: A simple matter of life and death-the trials of postnatal Beta-cell mass regulation. Int J Endocrinol 2012;2012:516718
60. Parkash V, Lindholm P, Peranen J, Kalkkinen N, Oksanen E, Saarma M, Leppanen VM, Goldman A: The structure of the conserved neurotrophic factors MANF and CDNF explains why they are bifunctional. Protein Eng Des Sel 2009;22:233-241
61. Boslem E, Meikle PJ, Biden TJ: Roles of ceramide and sphingolipids in pancreatic beta-cell function and dysfunction. Islets 2012;4:177-187
62. Chen L, Feng L, Wang X, Du J, Chen Y, Yang W, Zhou C, Cheng L, Shen Y, Fang S, Li J, Shen Y: Mesencephalic astrocyte-derived neurotrophic factor is involved in inflammation by negatively regulating the NF-kappaB pathway. Sci Rep 2015;5:8133
63. Neves J, Zhu J, Sousa-Victor P, Konjikusic M, Riley R, Chew S, Qi Y, Jasper H, Lamba DA: Immune modulation by MANF promotes tissue repair and regenerative success in the retina. Science 2016;353:aaf3646
64. Lee AH, Heidtman K, Hotamisligil GS, Glimcher LH: Dual and opposing roles of the unfolded protein response regulated by IRE1alpha and XBP1 in proinsulin processing and insulin secretion. Proc Natl Acad Sci U S A 2011;108:8885-8890
65. Szabat M, Page MM, Panzhinskiy E, Skovso S, Mojibian M, Fernandez-Tajes J, Bruin JE, Bround MJ, Lee JT, Xu EE, Taghizadeh F, O'Dwyer S, van de Bunt M, Moon KM, Sinha S, Han J, Fan Y, Lynn FC, Trucco M, Borchers CH, Foster LJ, Nislow C, Kieffer TJ, Johnson JD: Reduced Insulin Production Relieves Endoplasmic Reticulum Stress and Induces beta Cell Proliferation. Cell Metab 2016;23:179-193
66. Yang S, Yang H, Chang R, Yin P, Yang Y, Yang W, Huang S, Gaertig MA, Li S, Li XJ: MANF regulates hypothalamic control of food intake and body weight. Nat Commun 2017;8:579

FIGURE LEGENDS

Figure 1. MANF is specifically expressed in the β-cell of the islets of Langerhans.

(A-D) Immunohistochemical localization of MANF protein in pancreatic primordium at E13.5 in *Manf* $^{+/+}$ embryo **(A)**, and in adult *Manf* $^{+/+}$ mouse pancreas **(B),** using sections from E13.5 *Manf* $^{-/-}$ embryo **(D)**, and adult *Manf* $^{-/-}$ mouse pancreas **(D)** as specificity controls for anti-MANF antibody (Icosagen). Scale bar, 50 μm.

(E) Quantitative RT-PCR analysis for *Manf* mRNA levels in islets of Lagerhans isolated from *Manf* $^{+/+}$ mice (n = 6) and exocrine tissue (n = 3) from *Manf* $^{+/+}$ mice at P56. Values represent mean ± SEM, *p < 0.05, **p < 0.01, ***p< 0.001, ns. –not significant.

(F) Western blot analysis of lysates from isolated islets confirms that MANF protein is not expressed in islets from *Manf* $^{-/-}$ mice. Recombinant human MANF protein (15 ng MANF) was used as positive control and anti-GAPDH antibody for normalization of total protein content.

(G-V) Double immunohistochemistry analysis with anti-MANF antibody **(H, L, P, T)** and antibodies against other islet hormones, insulin **(G)**, and somatostatin **(K),** glucagon **(O),** PP **(S)**. MANF (red) was co-expressed with insulin in β-cells (green) and weakly with somatostatin in δ-cells (green). Almost no MANF signal was detected in α-(green) or PP (green) cells. Very weak or no MANF positive staining was observed in *Manf* $^{-/-}$ pancreatic islets **(J, N, R, V).** Cell nuclei were labelled with DAPI (blue). Scale bar, 10 μm.

(W-Z) Representative confocal laser scanning microscopy images of primary mouse islet β-cells double-stained with anti-MANF (red) and anti-PDI (protein disulphide isomerase, ER marker, green), anti-GM130 (Golgi marker, green), anti-insulin (green) or anti-GRP78 (green) antibodies. Scale bar, 8 μm. Quantitative co-localization analysis based on Pearson's correlation coefficient and Mander's coefficients (shown in the Supplementary Table 2) revealed high co-localization of MANF with ER marker PDI and insulin, moderate co-localization with GRP78 and no co-localization of MANF with Golgi marker GM130.

Figure 2. MANF expression in β-cells is important for restoring the β-cell mass.

(A) Insulin **(A, D, G)**, glucagon **(B, E, H)** and MANF **(C, F, I)** immunohistochemistry on pancreas sections from P56 *Pdx-1Cre* $^{+/-}$::*Manf* $^{fl/fl}$ mice. Scale bar, 50 μm.

(J-O) Double immunohistochemistry with anti-insulin (green) **(J, K)** and anti-MANF antibodies (red) **(L, M)** show mosaic **(L)** or no **(M)** MANF expression in P56 *Pdx-1Cre* $^{+/-}$::*Manf* $^{fl/fl}$ mice. Cell nuclei in merged picture **(N-O)** labelled with DAPI (blue). Scale bar, 20μm.

(P) β-cell mass in P56 *Pdx-1Cre* $^{+/-}$::*Manf* $^{fl/fl}$ mice positively correlates with the number of MANF positive insulin-positive cells, *n* = 15.

(Q) The number of MANF positive insulin-positive cells negatively correlates with the blood glucose levels in P56 *Pdx-1Cre* $^{+/-}$::*Manf* $^{fl/fl}$ mice, *n* = 18.

(R) The fraction of MANF-positive insulin-positive β-cells negatively correlates with the number of TUNEL-positive β-cells in P56 *Pdx-1Cre*$^{+/-}$::*Manf*$^{fl/fl}$ mice, *n* = 11.

Figure 3. MANF expression is required for maintaining the β-cell mass.

(A-C) Quantitative RT-PCR for mRNA levels of β cell-specific genes *Glut2*, *Ins1/2*, *Pdx-1*, *Gck* and *MafA* in islets from P1 **(A)**, P14 **(B)**, and P56 **(C)** pancreases, n = 6-11 per group .

(D-E) Quantitative RT-PCR PCR analysis of UPR genes *Atf4*, *Grp78*, *Chop*, spliced *(sp)Xbp1, total (t)Xbp*, and *Atf6a* and *Atf6β* in P1 **(D)** and P14 **(E)** *islets from Pdx-1Cre*$^{+/-}$::*Manf*$^{fl/fl}$ and *Manf*$^{fl/fl}$ mice. *n* = 6-11 per group.

(F-N) Double immunohistochemistry of MANF (red) **(I-K)** and GLUT2 (green) **(F-H)** in pancreatic sections from *Manf*$^{fl/fl}$ **(F, I, L)** and *Pdx-1Cre*$^{+/-}$::*Manf*$^{fl/fl}$ **(G-H, J-K, M-N)** mice at P56. Cell nuclei were labelled with DAPI (blue). Scale bar, 10 μm.

Values represent mean ± SEM, **p* < 0.05, ***p* < 0.01, ****p*< 0.001.

Figure 4. Effects of MANF *in vitro*

(A) Recombinant MANF protein increases proliferation of β-cells from aged 15-month-old female C57BL/6 Rcc mice after 5 days in culture. *n* =quantified from 4-6 wells per group. The proliferative effect of MANF in a second experiment using 15-month-old female Hsd:ICR(CD-1) mice was 0.44 ± 0.067% compared to 0.25% ± 0.034% in control islets showing a similar significant increase in β-cell proliferation in the MANF-treated islets (data not shown).

(B-J) Double immunohistochemistry of insulin **(B, E, H)** and Edu **(C, F, I).** Cell nuclei were labelled with DAPI (blue). Scale bar, 50 μm.

(K-N) Quantitative RT-PCR PCR analysis of UPR genes *Manf, Grp78*, spliced *(sp)Xbp1* and *total (t)Xbp* in primary mouse pancreatic islets treated with 30mM (+) glucose or non-treated (-) without (-) or with recombinant human MANF (+) overnight in RPMI medium supplemented with 0.5% BSA. *n* = 4-5 wells per group.

Values represent mean ± SEM, *p < 0.05, **p < 0.01, ***p< 0.001.

Figure 5. Deletion of MANF exclusively from adult pancreatic β-cells results in diabetes in *MIP-1Cre^{ERT}::Manf$^{fl/fl}$* mice.

(A) Body weights of *MIP-1Cre^{ERT}::Manf$^{fl/fl}$* and *Manf$^{fl/fl}$* animals 4 weeks after last TMX injection, *n* =11-12 mice per group, both genders.

(B) *Ad libitum*-fed blood glucose levels measured 4 weeks after last TMX injection, *n* = 11-12 mice per group, both genders.

(C) Serum insulin levels measured 4 weeks after TMX injection from *ad libitum*-fed mice, *n* = 11-12 mice per group, both genders.

(D) Blood glucose levels measured after intraperitoneal glucose (2 g/kg) injection, *n* = 5-12 mice per group.

(E-G) *In vitro* insulin release from islets in response to low glucose (1.67 mmol/l; G1.67), high glucose (16.7 mmol/l; G16.7), and high glucose with IBMX (1 mmol/l), normalized to islet DNA content after 1 hr **(E)**.Total insulin content normalized to islet DNA content **(F)**. In vitro glucose-stimulated insulin release compared to total islet insulin content **(G)**, *n* = islets from six pancreases/group.

(H-M) Recombination efficiency is varying in individual mouse showing different amount of MANF expressing β-cells by double fluorescence immunohistochemistry in pancreatic sections of *MIP-1Cre^{ERT}::Manf$^{fl/fl}$* mice injected with TMX with anti-insulin **(L)** (green) and anti-MANF antibodies **(M)** (red). Cell nuclei were labelled with DAPI (blue). Scale bar, 50 μm.

(N-Q) Immunohistochemical analysis of insulin- **(N, O)** and glucagon-positive **(P, Q)** cells in pancreatic sections reveals morphological changes in the islets of from *MIP-1Cre^{ERT}::Manf$^{fl/fl}$* injected with TMX compared to those injected with oil. Scale bar, 50 μm.

(R) The β-cell mass is significantly reduced in P90 *MIP-1Cre^{ERT}::Manf$^{fl/fl}$* mice injected with TMX, compared to the β-cells mass in *MIP-1Cre^{ERT}::Manf$^{fl/fl}$* mice injected oilmice, *n* = 4-5 mice per group, both genders.

(S) β-cell proliferation assessed by Ki67 and insulin staining, *n* =6 mice per group.

(T) β-cell apoptosis assessed by TUNEL and insulin staining, *n* =6 mice per group.

Mean ± SEM, *p < 0.05, **p < 0.01, ***p< 0.001 versus the corresponding control.

Figure 6. MANF expression in β-cells is essential for maintaining the adult β-cell mass.

(A) Quantitative RT-PCR for mRNA levels of β cell-specific genes *Glut2*, *Ins1/2*, *Pdx-1*, *Gck* and *MafA* in islets from P90 *MIP-1Cre^{ERT}::Manf$^{fl/fl}$* injected with oil (white bars) and tamoxifen (black bars). *n* = islets from 7-9 mice per group.

(B) Quantitative RT-PCR PCR analysis of UPR genes *Atf4*, *Grp78*, *Chop*, s*Xbp1, tXbp*, and *Atf6a* and *Atf6β* in islets from *MIP-1Cre^{ERT}::Manf$^{fl/fl}$* injected with oil (white bars) and tamoxifen (black bars). *n* =islets from 7-9 mice per group.

(C-H) Double immunohistochemistry of MANF (red) **(D, G)** and GLUT2 (green) **(C, F)** in pancreatic sections from P90 *MIP-1Cre^{ERT}::Manf$^{fl/fl}$* mice injected with oil and tamoxifen. Scale bar, 10 μm.

(I-N) Double immunohistochemistry of PDX1 (red) **(J, M)** and insulin (green) **(I, L)** in pancreatic sections from *MIP-1Cre^{ERT}::Manf$^{fl/fl}$* injected with oil or tamoxifen. Scale bar, 10 μm.
Mean ± SEM, *p < 0.05, **p < 0.01, ***p< 0.001 versus the corresponding control.

Figure 7. Insights in MANF mechanism of action

(A-P) Cell signalling pathways in islet β–cells from 4-5-week-old *Manf$^{-/-}$* and *Manf$^{+/+}$* mice in the presence or absence of recombinant MANF **(A, E, G, K, M, O**). Western blotting with indicated antibodies on islet lysates from *Manf$^{-/-}$* and *Manf$^{+/+}$* mice, non-treated (-) or treated (+) with recombinant MANF. Quantified intensities of western blot bands of phospho-AKT (Ser 473) compared to the total amount of AKT **(B)**, phospho-ERK1/2 to total ERK1/2 **(F)**, phospho-NF-κB p65 (Ser536) to total NF-κB p65 **(H)**, phospho-c-Jun (Ser63) to total c-Jun **(L)**, phospho-p38 to total p38 **(N)** and iNOS compared to GAPDH (glyceraldehyde 3-phospate dehydrogenase) **(P)**. *n* =2-3 wells per group. Quantitative real-time PCR analysis of *Trib3* expression **(C, D)** in islets isolated from *Manf$^{fl/fl}$* and *Pdx-1Cre$^{+/-}$::Manf$^{fl/fl}$* mice at postnatal days 1 (P1) and 14 (P14) **(C)** and from oil and TMX-injected *MIP-1Cre^{ERT}::Manf$^{fl/fl}$* mice **(D)**, *n* = islets from 4-6 mice per group. Quantitative real-time PCR analysis of *Bcl10* mRNA expression **(I, J)** in islets isolated from *Manf$^{fl/fl}$* and *Pdx-1Cre$^{+/-}$::Manf$^{fl/fl}$* mice at postnatal days 1(P1) and 14(P14) **(I)** and from oil and TMX-injected *MIP-1Cre^{ERT}::Manf$^{fl/fl}$* mice (J), *n* = islets from 4-6 mice per group. ns., non-significant. Mean ± SEM, *p < 0.05, **p < 0.01, ***p< 0.001 versus the corresponding control.

(Q) A link between ER stress and inflammation in MANF-deficient mouse pancreatic β-cells. MANF deficiency in β-cells leads to ER stress and activation of all three UPR branches, ATF6, PERK and IRE1α. Transcription factor ATF4, which escapes the translational inhibition induced by pEIF2α in the PERK pathway, increases *Trib3* expression. TRIB3 is known to block AKT

phosphorylation and thereby inhibits insulin signalling and β-cell cycle progression (62). Expression of CHOP, a pro-apototic transcription factor is induced by both cleaved ATF6 and ATF4. IRE1α activation results in activation of JNKs, NF-κB and p38MAPK inflammatory signalling cascades contributing to the increased expression of several pro-apoptotic genes including *Bcl10*, which is a known inducer of apoptosis and regulator of NF-κB. Nuclear NF-κB activation leads to increase iNOS production which contributes to increased NO production. NO has been found to inhibit the SERCA-2b pump and thereby contributes to depletion of Ca^{2+} from the ER leading to increased ER stress (46). **Abbreviations**: ER, endoplasmic reticulum; ATF, activating transcription factor; PERK, protein kinase R-like endoplasmic reticulum kinase; IRE1, inositol-requiring enzyme; NF-κB, nuclear factor κ-light-chain-enhancer of activated B cells; JNK, c-Jun N-terminal kinases, iNOS, inducible nitric oxide synthase: NO, nitric oxide; BCL10, B-cell lymphoma/leukemia 10; IKB, inhibitor if κB kinases; SERCA2b, sarcoplasmic/endoplasmic reticulum calcium ATPase.

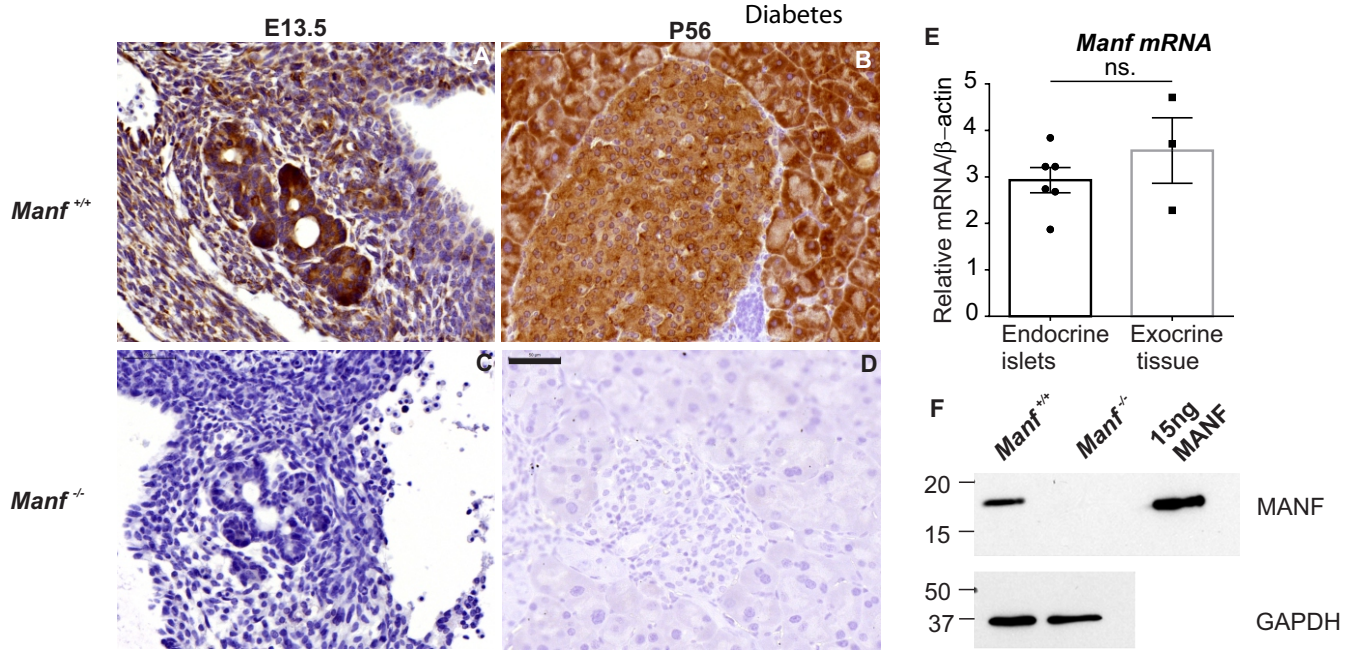
E13.5
P56
A
B
C
D
Manf +/+
Manf -/-
E
Manf mRNA
ns.
Relative mRNA/β–actin
5
4
3
2
1
0
Endocrine islets
Exocrine tissue
F
Manf +/+
Manf -/-
15ng MANF
20
15
50
37
MANF
GAPDH

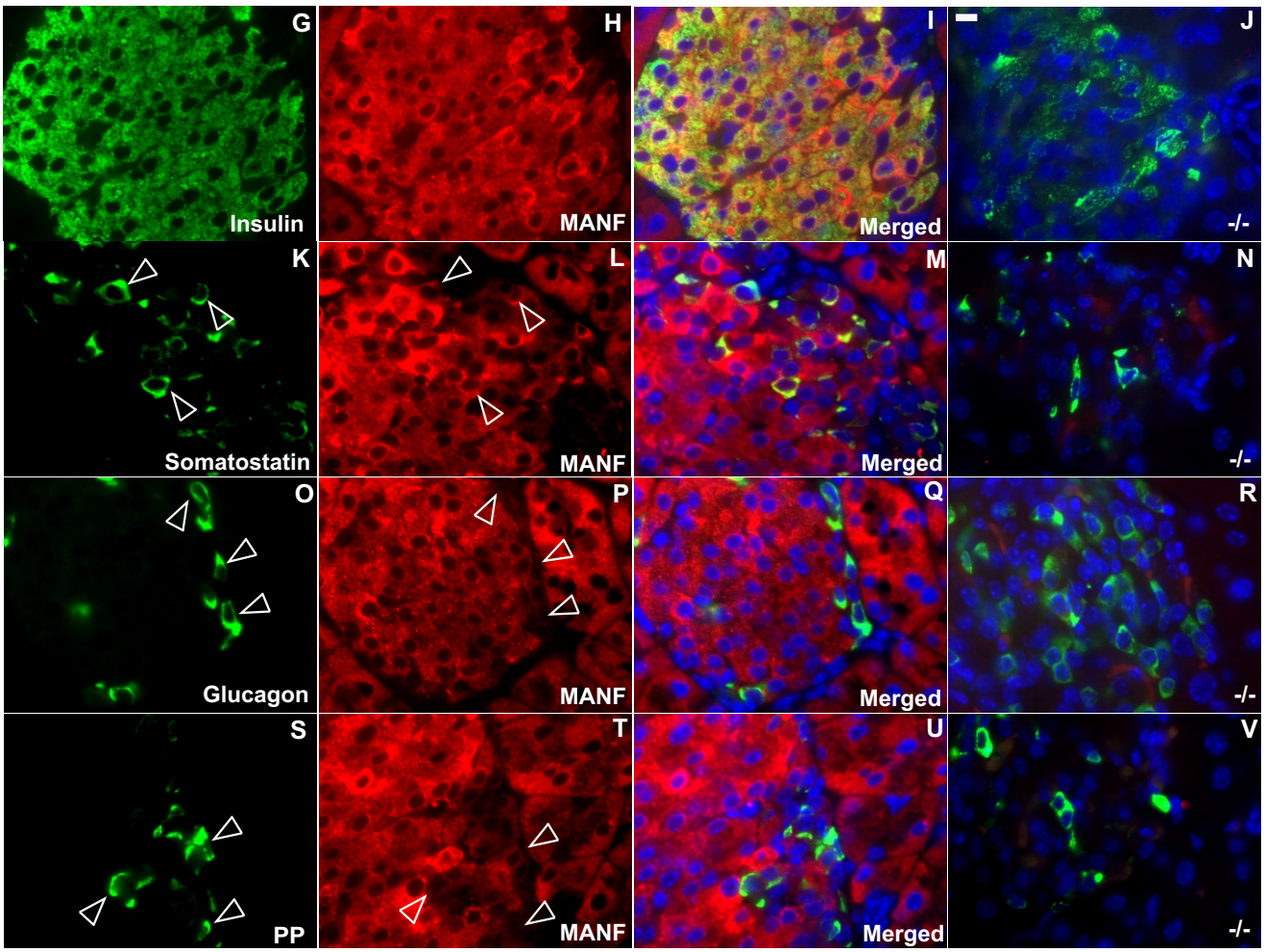
G
Insulin
H
MANF
I
Merged
J
-/-
K
Somatostatin
L
MANF
M
Merged
N
-/-
O
Glucagon
P
MANF
Q
Merged
R
-/-
S
PP
T
MANF
U
Merged
V
-/-

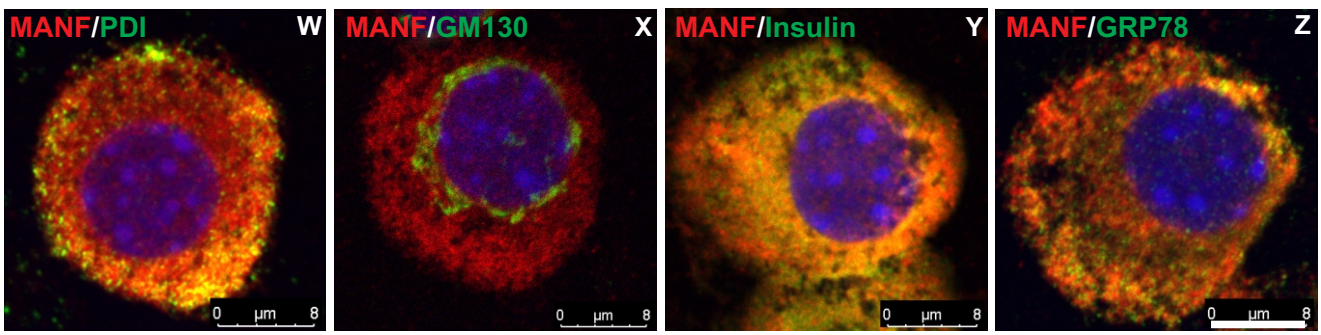
MANF/PDI
W
MANF/GM130
X
MANF/Insulin
Y
MANF/GRP78
Z
0 µm 8

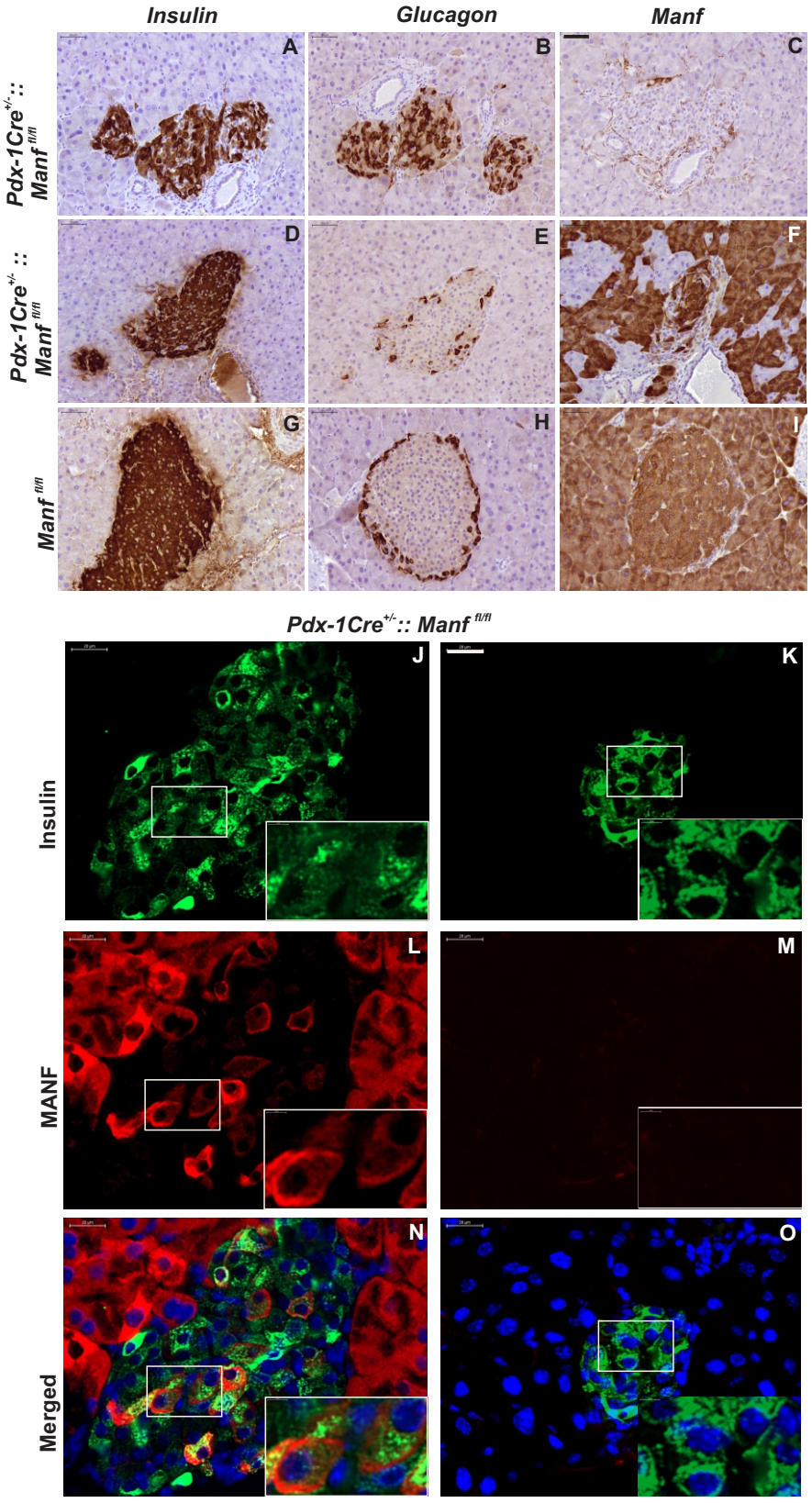
Insulin
Glucagon
Manf
A
B
C
D
E
F
G
H
I
Pdx-1Cre+/- :: Manf fl/fl
Pdx-1Cre+/- :: Manf fl/fl
Manf fl/fl
Pdx-1Cre+/- :: Manf fl/fl
J
K
L
M
N
O
Insulin
MANF
Merged

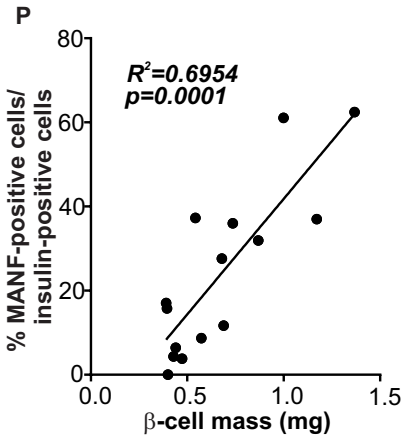
P
R2=0.6954
p=0.0001
% MANF-positive cells/ insulin-positive cells
β-cell mass (mg)

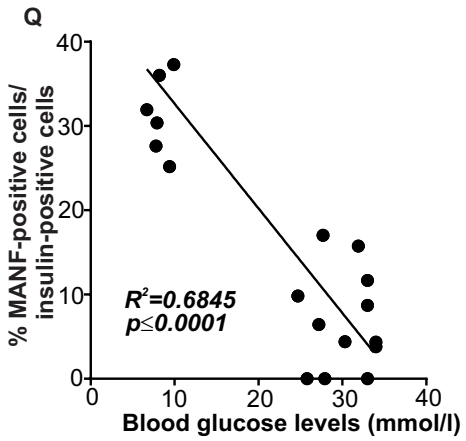
Q
R2=0.6845
p≤0.0001
% MANF-positive cells/ insulin-positive cells
Blood glucose levels (mmol/l)

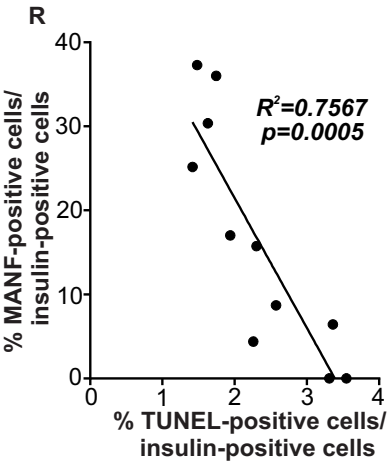
R
R2=0.7567
p=0.0005
% MANF-positive cells/ insulin-positive cells
% TUNEL-positive cells/ insulin-positive cells

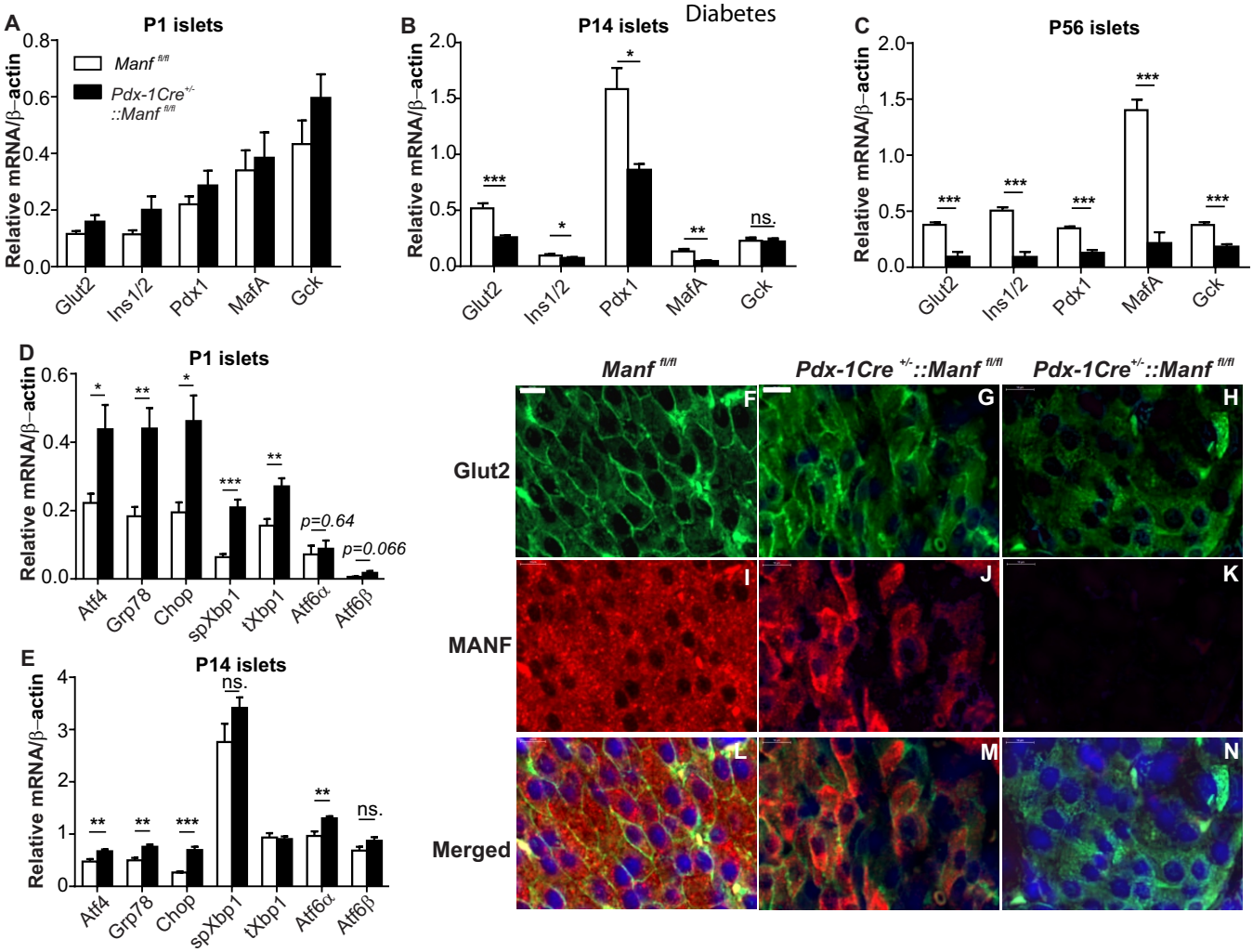
A
P1 islets
Manf fl/fl
Pdx-1Cre+/- ::Manf fl/fl
Relative mRNA/β–actin
Glut2
Ins1/2
Pdx1
MafA
Gck
B
P14 islets
C
P56 islets
D
P1 islets
Atf4
Grp78
Chop
spXbp1
tXbp1
Atf6α
Atf6β
p=0.64
p=0.066
E
P14 islets
ns.
Manf fl/fl
Pdx-1Cre +/-::Manf fl/fl
Glut2
MANF
Merged
F
G
H
I
J
K
L
M
N

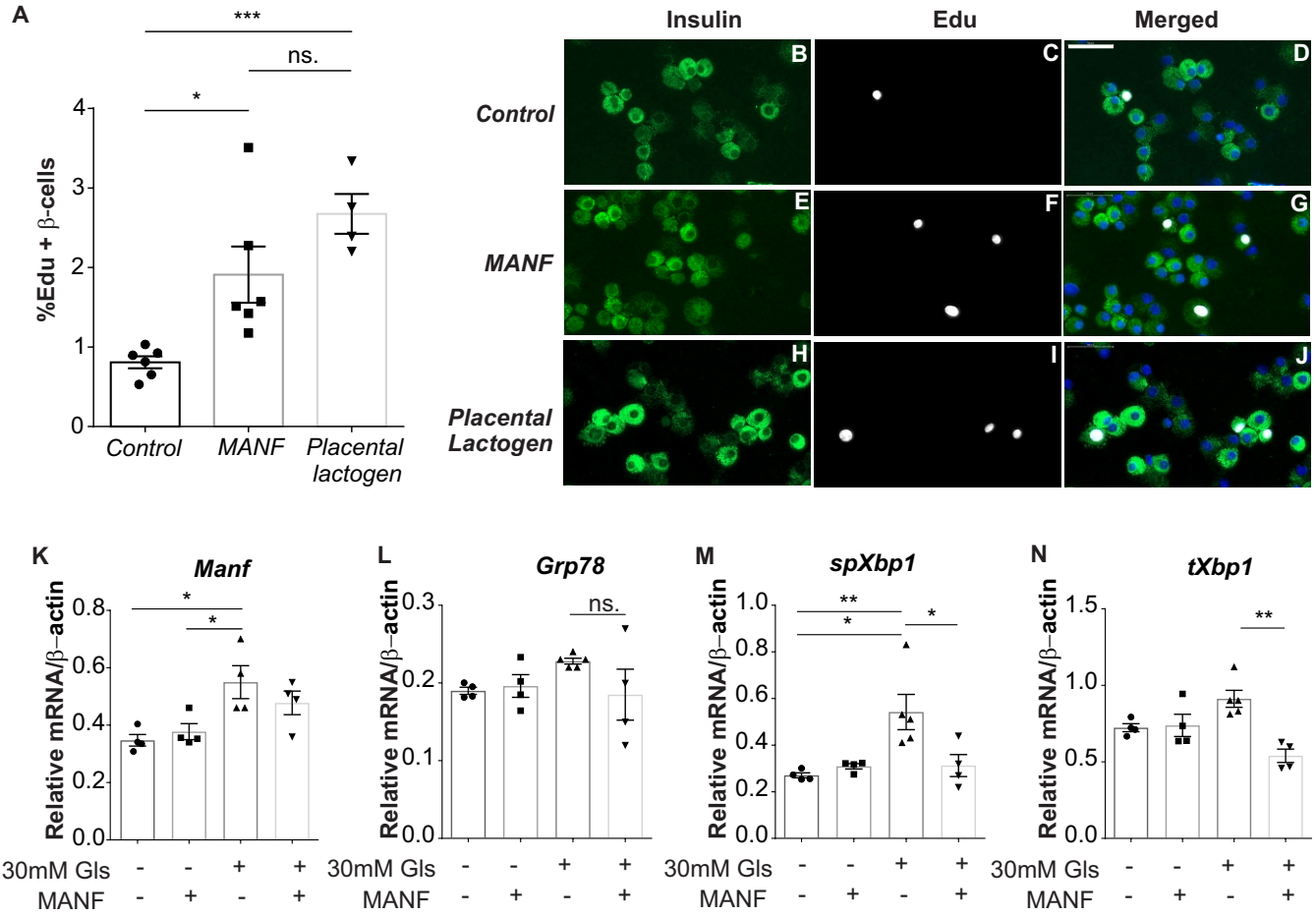
A
***
ns.
*
%Edu + β-cells
Control
MANF
Placental lactogen
Insulin
Edu
Merged
Control
MANF
Placental Lactogen
B
C
D
E
F
G
H
I
J
K
Manf
Relative mRNA/β-actin
L
Grp78
ns.
M
spXbp1
**
N
tXbp1
30mM Gls
MANF

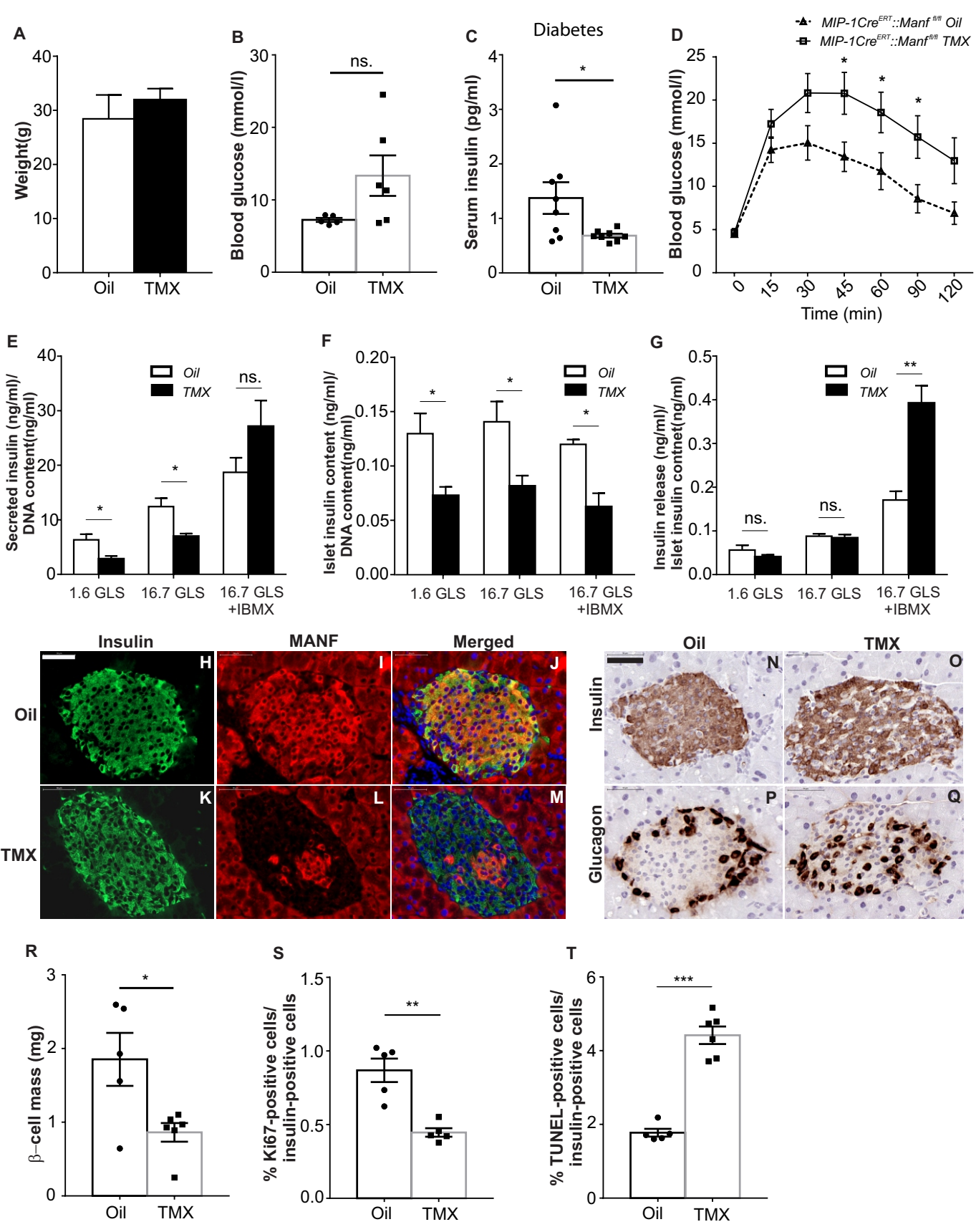
A
Weight(g)
Oil
TMX
B
Blood glucose (mmol/l)
ns.
C
Diabetes
Serum insulin (pg/ml)
D
MIP-1Cre^ERT::Manf fl/fl Oil
MIP-1Cre^ERT::Manf fl/fl TMX
Blood glucose (mmol/l)
Time (min)
E
Secreted insulin (ng/ml)/ DNA content(ng/ml)
1.6 GLS
16.7 GLS
16.7 GLS +IBMX
F
Islet insulin content (ng/ml)/ DNA content(ng/ml)
G
Insulin release (ng/ml)/ Islet insulin contnet(ng/ml)
Insulin
MANF
Merged
Oil
TMX
H
I
J
K
L
M
N
O
P
Q
Glucagon
R
β–cell mass (mg)
S
% Ki67-positive cells/ insulin-positive cells
T
% TUNEL-positive cells/ insulin-positive cells

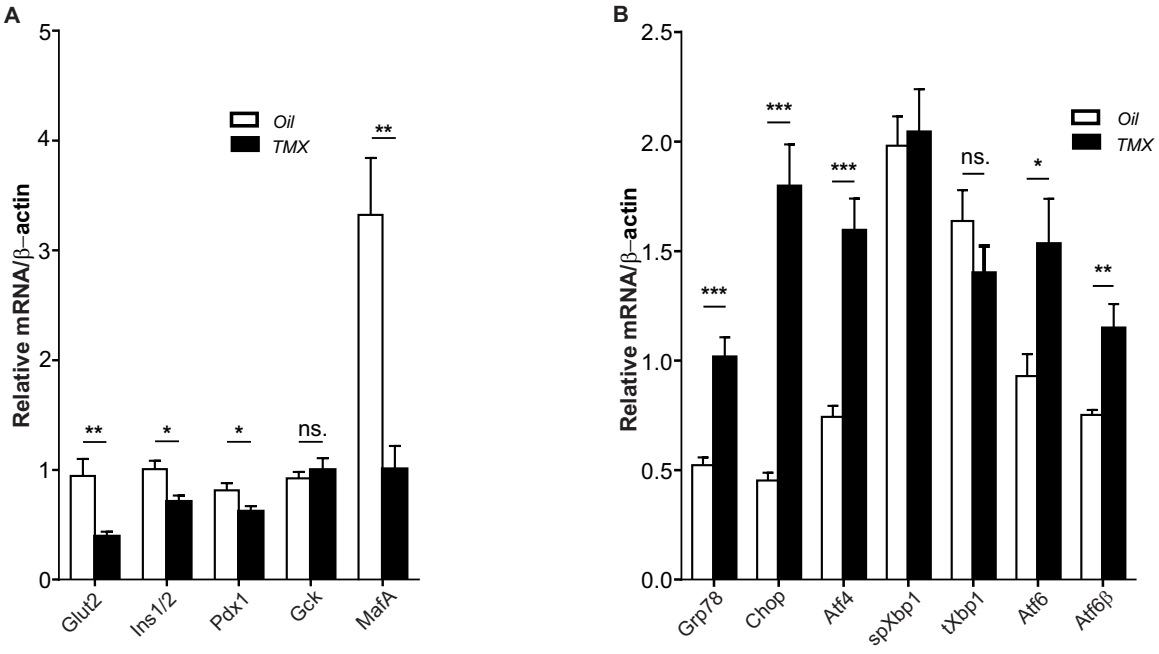
A
Relative mRNA/β–actin
Oil
TMX
Glut2
Ins1/2
Pdx1
Gck
MafA
B
Relative mRNA/β–actin
Oil
TMX
Grp78
Chop
Atf4
spXbp1
tXbp1
Atf6
Atf6β
ns.

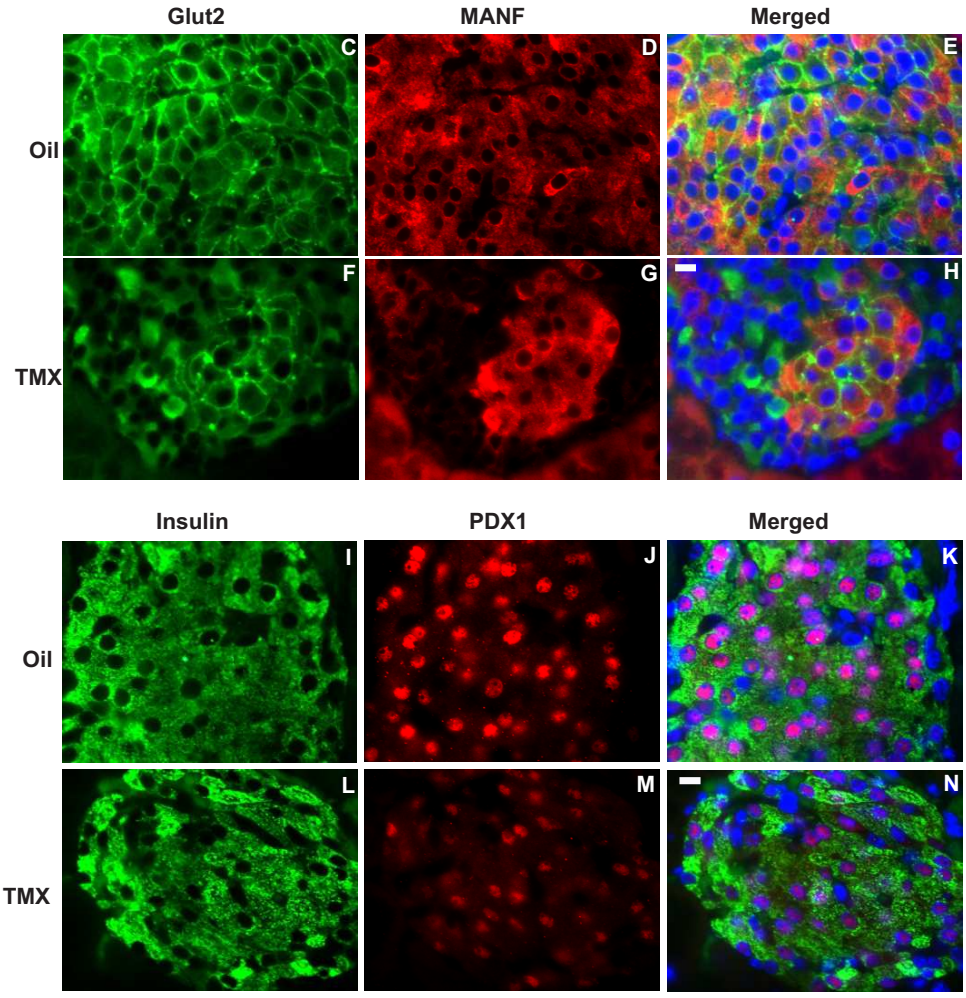
Glut2
MANF
Merged
Oil
TMX
C
D
E
F
G
H
Insulin
PDX1
Merged
Oil
TMX
I
J
K
L
M
N

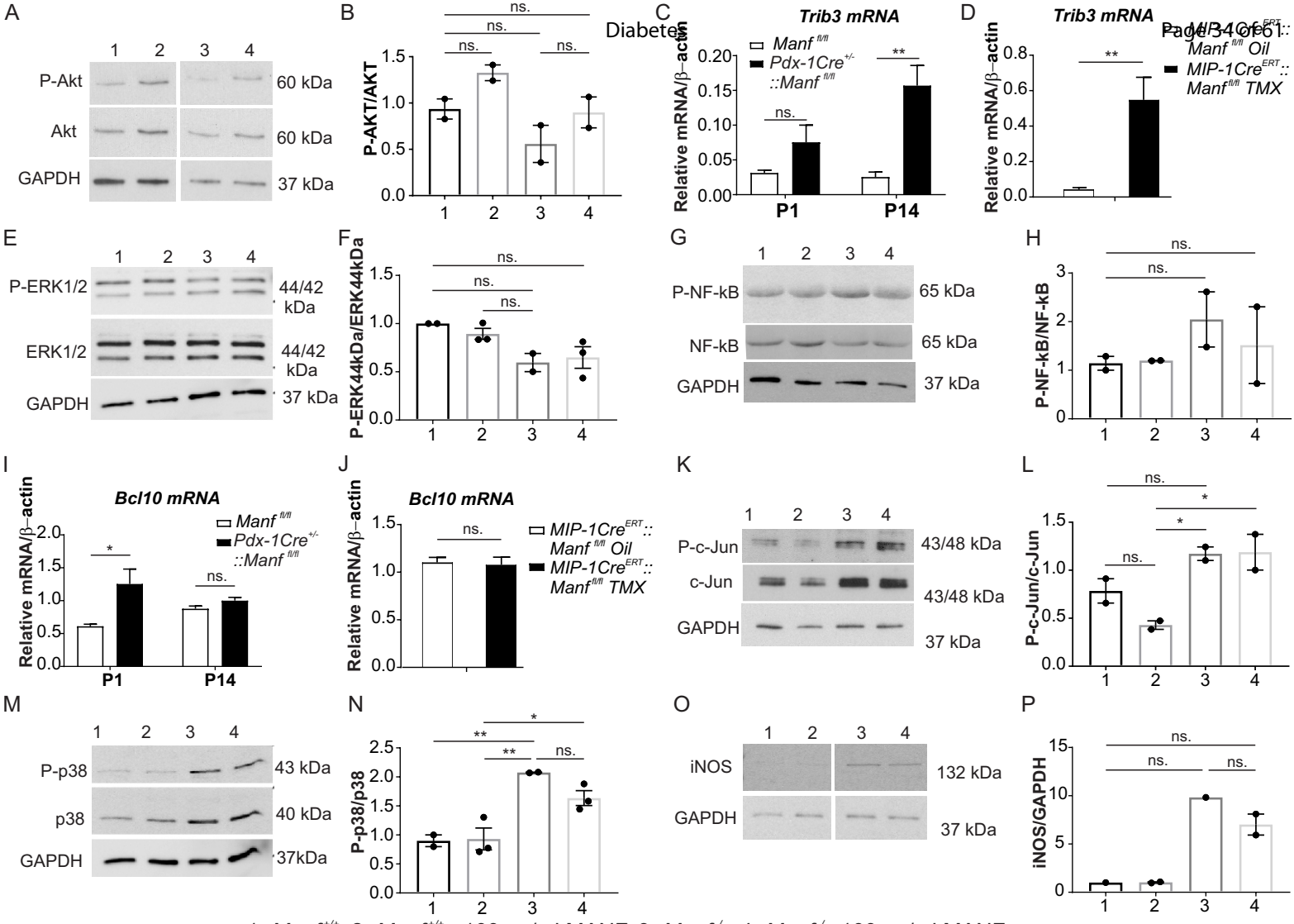

1. *Manf*$^{+/+}$, 2. *Manf*$^{+/+}$+ 100 ng/ml MANF, 3. *Manf*$^{-/-}$, 4. *Manf*$^{-/-}$+100 ng/ml MANF

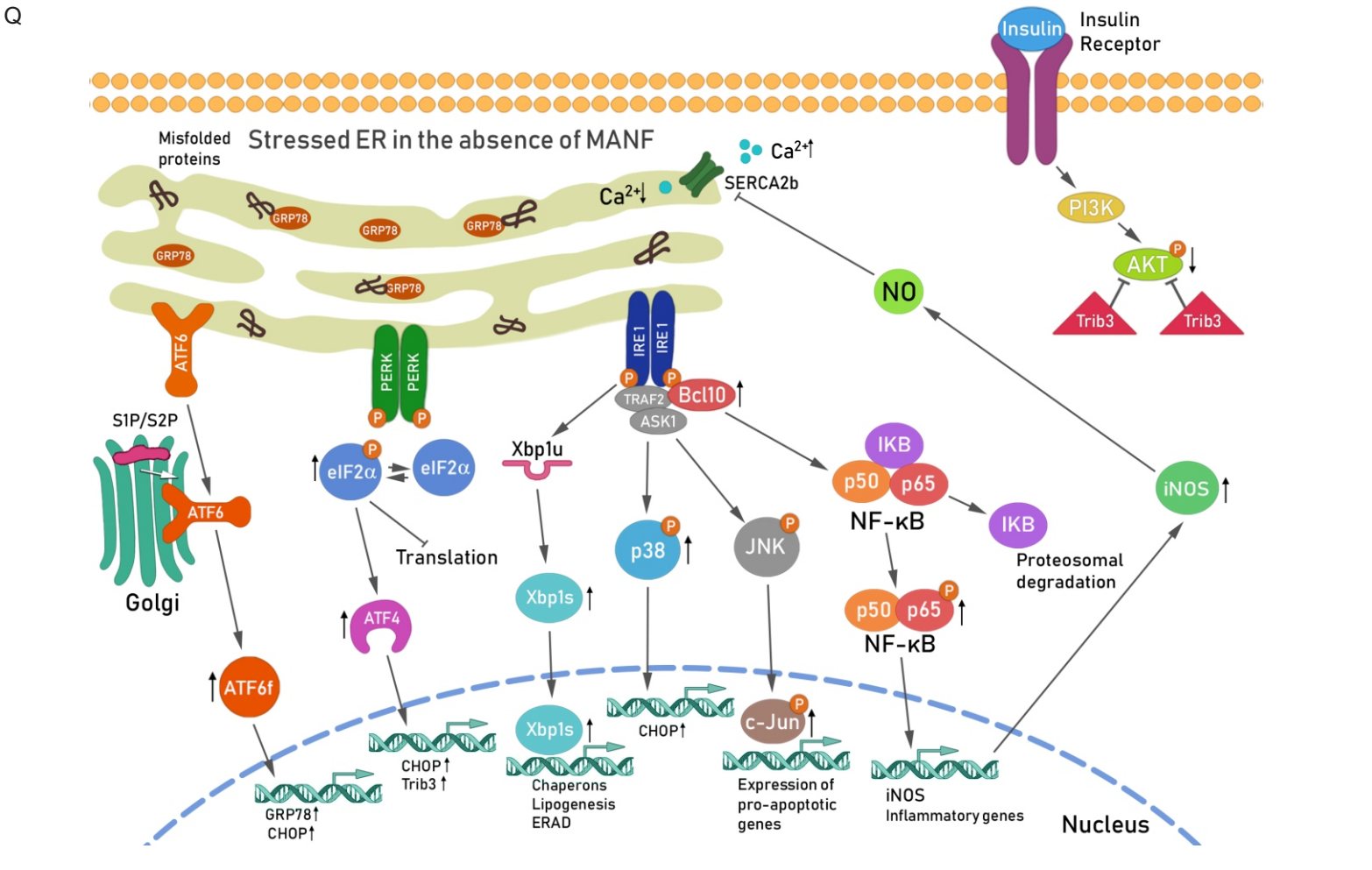

Supplemental text

Analysis of Pdx-1 Cre recombinase activity

Pdx-1 Cre recombinase activity was examined by crossing *Pdx-1Cre*$^{+/-}$ mice to tdTomato reporter mice. We detected Cre-mediated tdTomato expression in the pancreas, but also in duodenum and liver at different embryonic and postnatal stages (Supplementary Fig. 3.1K-DD). In embryonic and early postnatal pancreas development MANF was found to be expressed in most cells with the highest expression in endocrine cells (Supplementary Fig. 3.1K-M, O-Q).

Pancreas-specific ablation of MANF leads to diabetes in mice

The absence of MANF from conventional *Manf* $^{-/-}$ mice and from the pancreases of conditional *Pdx-1Cre*$^{+/-}$::*Manf*$^{fl/fl}$ mice results in diabetes (1). In contrast to *Manf*$^{-/-}$ mice, the *Pdx-1Cre*$^{+/-}$::*Manf*$^{fl/fl}$ mice do not show growth retardation (Supplementary Fig. 2.1B), suggesting that MANF-removal from other cells rather than β-cells results in the growth defect in conventional *Manf*$^{-/-}$ mice. A slight reduction in weight was observed in P56 *Pdx-1Cre*$^{+/-}$::*Manf*$^{fl/fl}$ mice, when animals already were overtly diabetic. In contrast to *Manf*$^{-/-}$ mice, *Pdx-1Cre*$^{+/-}$::*Manf*$^{fl/fl}$ mice developed diabetes later. Blood glucose and serum insulin levels were within the normal range in P1 and P14 random fed animals (Supplementary Fig. 2.1C-D). However, severe hyperglycaemia and significant reduction in serum insulin levels were observed in random fed P56 conditional mice (Supplementary Fig. 2.1C-D). Glucose tolerance test revealed impaired glucose clearance and a trend toward reduced glucose stimulated insulin secretion in P56 *Pdx-1Cre*$^{+/-}$::*Manf*$^{fl/fl}$ compared to controls (Supplementary Fig. 2.1E-F). As reported for *Manf*$^{-/-}$ mice (1), insulin tolerance test performed on P42 *Pdx-1Cre*$^{+/-}$::*Manf*$^{fl/fl}$ conditional mice revealed intact insulin sensitivity (Supplementary Fig. 2.1G).

Histological analysis of pancreases revealed marked loss of islet architecture and reduced insulin staining in P56 *Pdx-1Cre*$^{+/-}$::*Manf*$^{fl/fl}$ mice (Supplementary Fig. 2.1I-N, 2.1O-T). Quantification of the β-cell mass demonstrated no changes at P1. However, by P14 the β-cell mass was reduced in *Pdx-1Cre*$^{+/-}$::*Manf*$^{fl/fl}$ pancreases compared to controls (Supplementary Fig. 2.1U). Consequently, islet-cell mass in P56 *Pdx-1Cre*$^{+/-}$::*Manf*$^{fl/fl}$ pancreases was reduced (data not shown), indicating β-cell loss. Consistent with our data with global *Manf*$^{-/-}$ mice, lack of MANF from the pancreas resulted in a significantly reduced number of Ki67 positive β-cells starting at P14 (Supplementary Fig. 2.1W). The reduction of the β-cell mass was also accompanied by increased levels of β-cell

apoptosis in P14 and P56 pancreases from conditional mice quantified by TUNEL assay (Supplementary Fig. 2.1X, 2.1Y-DD).

Supplemental Experimental Procedures

Animals and in vivo physiology

In brief, *Manf*$^{fl/fl}$ mice were produced by removing the β-galactosidase reporter cassette preceded by a strong splicing acceptor by crossing *Manf*$^{+/-}$ mice with ubiquitous Flp expressing *CagFlp* mice (1) and (Supplementary Fig. 2.1A).

Pdx-1Cre recombinase activity was evaluated by crossing *Pdx-1Cre* mice with *Rosa26-tdTomato*$^{fl/Stop/fl}$ reporter mice (Jackson Laboratories, Stock 007914).

Collected blood samples from the mice were assayed for glucose (Accucheck Aviva Glucometer; Roche Diagnostics) and sera for insulin (ultrasensitive mouse insulin ELISA; Crystal Chem) measurements. DNA isolation and genotyping of mice were carried out as described previously (1,2) and in Supplementary Data.

Genotyping primers and expected PCR products

DNA was isolated from ear-marks and genotyping was carried out. For *MIP-1Cre*^{ERT} mice the following primers were used: Forward (transgene) 5'-TGGACTATAAAGCTGGTGGGCAT-3', Reverse (transgene) 5'-TGCGAACCTCATCACTCGT-3', Internal Positive Control Forward 5'-CTAGGCCACAGAATTGAAAGATCT-3', Internal Positive Control Reverse 5'-GTAGGTGGAAATTCTAGCATCATCC-3' (PCR products: Transgene = ~230 bp, Internal positive control = 324 bp). For *Rosa26-tdTomato*$^{fl/Stop/fl}$ reporter mice the following primers were used: Wild type Forward 5'-AAGGGA GCT GCA GTG GAG TA-3', Wild type Reverse 5'-CCG AAA ATC TGT GGG AAG TC-3', Mutant Reverse 5'-GGCATTAAAGCAGCGTATCC-3', Mutant Forward 5'-CTGTTCCTG TACGGCATGG-3' (PCR products: Mutant = 196 bp, Heterozygote = 297 bp and 196 bp, Wild type = 297 bp).

Histological Analysis

Islet-cell mass was assessed from pancreatic sections stained with anti-Chromogranin A antibody and quantified similarly to beta cell mass described previously (1).

For identification of LacZ activity cryosections were stained with X-gal solution as described previously (3).tdTomato expression was detected in cryosections as described previously (4) and followed by staining with anti-MANF antibody and DAPI.

Fluorescence or light microscopy images were captured with 3DHISTECH Panoramic 250 FLASH II digital slide scanner (Budapest, Hungary, with scanning service in the Institute of Biotechnology and in Research Programs Unit, Faculty of Medicine, University of Helsinki, Biocenter Finland) or Zeiss AxioImager M2 482 epifluorescence microscope equipped with 483 AxioCam HRm camera. Images were analysed with Pannoramic viewer program or acquired with the AxioVision4 software.

Subcellular localization analysis

Islets from C57BL/6Rcc pancreases were isolated and cultured overnight in the RPMI1649 medium supplemented with 10% Fetal Bovine Serum and a mixture of antibiotics. Next day islets were dissociated with Tryple™ Select Enzyme (Cat.number 12563011, Thermo Fisher Scientific, Waltham MA, USA), followed by centrifugation onto glass slides. Cells were fixed and stained for different primary antibodies (Supplementary Table 1). Appropriate secondary antibodies conjugated with Alexa Fluor® 488 or 568 (1:400, Molecular Probes, Life Technologies, Eugene, Oregon, USA) and DAPI (Vectorshield, Vector laboratories, Burlingame, USA) were used to visualize the labels.

Slides were imaged with PerkinElmer Opera Phenix high-content confocal microscope using Harmony 4.6 software (PerkinElmer), by using three lasers with excitation wavelengths 405nm, 488nm, and 568nm. 63x water immersion objective (NA 1.15) was used for imaging. The lateral pixel size was automatically set to 95nm and the distance between axial slices was set to 500nm according to the Nyquist criterion. Altogether 10-14 optical sections were recorded using 16-bit Andor Zyla CMOS camera (2160x2160 px). 125 and 49 fields-of-view were recorded from the first and second set of slides, respectively.

The colocalization analysis was performed in 3D for each cell separately. Densely packed and malformed cells were filtered out from the analysis. First, nuclei and cells were segmented from 2D maximum intensity projection images using Harmony software. Next, linear classifier was trained to classify cells into two classes: isolated and packed/malformed. Last, the 2D coordinates of isolated cells were exported from Harmony software. The rest of the analysis was carried out in 3D using BioImageXD software (5). Cells were segmented in 3D using combination of Hoechst and

MANF (568nm) channels. Only the cells overlapping with the exported 2D coordinates of isolated cells were used for colocalization analysis. For each cell, both Pearson correlation coefficient for overall signal correlation and Manders' coefficients (6) for channel specific colocalization were measured. The total number of analysed cells varied from 20 to 66.

Western Blotting

Western blotting analysis was performed using standard protocols and as described previously (1). For primary antibodies see Supplementary Table 1.

Islet isolation, In Vitro Insulin Release and In Vitro Islets experiments

Islet isolation and *in vitro* insulin release from islets were performed as described previously (1,7). In brief, pancreases were digested by collagenase P (Collagenase P; Roche Diagnostics) using standard protocol procedure and islets were purified from acinar tissues by handpicking them up under a microscope.

In order to test the effect of human recombinant MANF on ER stress in MANF-deficient islets we cultured isolated islets from 4-5-week old *Manf*$^{+/+}$ and *Manf*$^{-/-}$ mice for 24 h with or without MANF (1µg/ml, Icosagen) in 0.5% bovine serum albumin (BSA) in RPMI medium directly after islets isolation or with MANF (100ng/ml, Icosagen) for 3 days in 10% FBS RPMI medium, changing 2/3 of the medium into fresh every day.

To test the effect of MANF on mouse islets exposed to hyperglycaemia, isolated islets from 12-week-old C57BL/6Rcc mice were cultured in RPMI medium (glucose 11mM) supplemented with 0.5% BSA in the presence and absence of high levels of glucose (30mM) overnight with or without MANF 1µg/ml.

Analysis of Blood Samples by glucose tolerance test (GTT), insulin tolerance test (ITT), and by glucose challenge test (GTT).

Analysis of blood samples were performed as described previously (1).

RNA Isolation, Reverse Transcription, and Quantitative RT-PCR

RNA Isolation, reverse transcription, and quantitative real-time polymerase chain reaction (QPCR) were performed as described previously (1). Primer sequences for the gene expression studied by QPCR have been described previously (1). Other primer sequences: *mouse Bcl10* Forward 5'-AAA CTG GAG CAC CTC AAA GG -3', *mouse Bcl10* Reverse 5'-TCT CAT CGG AAT TGC ACC TA -3', *mouse Trib3* Forward 5'- CGC TTT GTC TTC AGC AAC TGT-3', *mouse Trib3* Reverse 5'-TCA TCT GAT CCA GTC ATC ACG -3'.

Serial block-face scanning electron microscopy (SB-EM)

The dissected tissues (<2 mm x 2 mm blocks) were stained using an enhanced staining protocol (8). First, the tissues were fixed with 2.5% glutaraldehyde and 2% formaldehyde, in 100 mM Na-cacodylate buffer (pH 7.4) supplemented with 2 mM $CaCl_2$ for 2 hours. Stained and dehydrated specimens were embedded into Durcupan ACM resin (Merck Sigma-Aldrich, Darmstadt, Germany), that was mixed according to the manufacturer's recommendations. The embedded tissue was trimmed to a pyramid and mounted onto a pin using conductive epoxy glue (model 2400; CircuitWorks, Kennesaw, GA). Finally, the sides of the pyramid were covered with silver paint (Agar Scientific Ltd, Stansted, UK), and the whole assembly was platinum coated using Quorum Q150TS (Quorum Technologies, Laughton, UK). SBEM data sets were acquired with an FEG-SEM Quanta 250 (Thermo Fisher Scientific, FEI, Hillsboro, OR), using a backscattered electron detector (Gatan Inc., Pleasanton, CA) with 2.5-kV beam voltage, a spot size of 3, and a pressure of 0.15-0.30 Torr. The block faces were cut with 40-nm increments and imaged with XY resolution of 16 nm per pixel.

References

1. Lindahl M, Danilova T, Palm E, Lindholm P, Voikar V, Hakonen E, Ustinov J, Andressoo JO, Harvey BK, Otonkoski T, Rossi J, Saarma M: MANF is indispensable for the proliferation and survival of pancreatic beta cells. Cell Rep 2014;7:366-375
2. Tamarina NA, Roe MW, Philipson L: Characterization of mice expressing Ins1 gene promoter driven CreERT recombinase for conditional gene deletion in pancreatic beta-cells. Islets 2014;6:e27685
3. Aird WC, Jahroudi N, Weiler-Guettler H, Rayburn HB, Rosenberg RD: Human von Willebrand factor gene sequences target expression to a subpopulation of endothelial cells in transgenic mice. Proc Natl Acad Sci U S A 1995;92:4567-4571

4. Morris LM, Klanke CA, Lang SA, Lim FY, Crombleholme TM: TdTomato and EGFP identification in histological sections: insight and alternatives. Biotech Histochem 2010;85:379-387
5. Kankaanpää P, Paavolainen L, Tiitta S, Karjalainen M, Päivärinne J, Nieminen J, Marjomäki V, Heino J, White DJ: BioImageXD: an open, general-purpose and high-throughput image-processing platform. Nature Methods 2012;9:683
6. Manders EMM, Verbeek FJ, Aten JA: Measurement of Colocalization of Objects in Dual-Color Confocal Images. J Microsc-Oxford 1993;169:375-382
7. Miettinen PJ, Ustinov J, Ormio P, Gao R, Palgi J, Hakonen E, Juntti-Berggren L, Berggren PO, Otonkoski T: Downregulation of EGF receptor signaling in pancreatic islets causes diabetes due to impaired postnatal beta-cell growth. Diabetes 2006;55:3299-3308
8. Deerinck TJ, Bushong E, Thor A. Ellisman MH. NCMIR methods for 3D EM: A new protocol for preparation of biological specimens for serial block-face SEM. Microscopy. 2010:6–8. https://ncmir.ucsd.edu/sbem-protocol

Supplementary figures and supplementary figure legends

Supplementary Figure 1.1

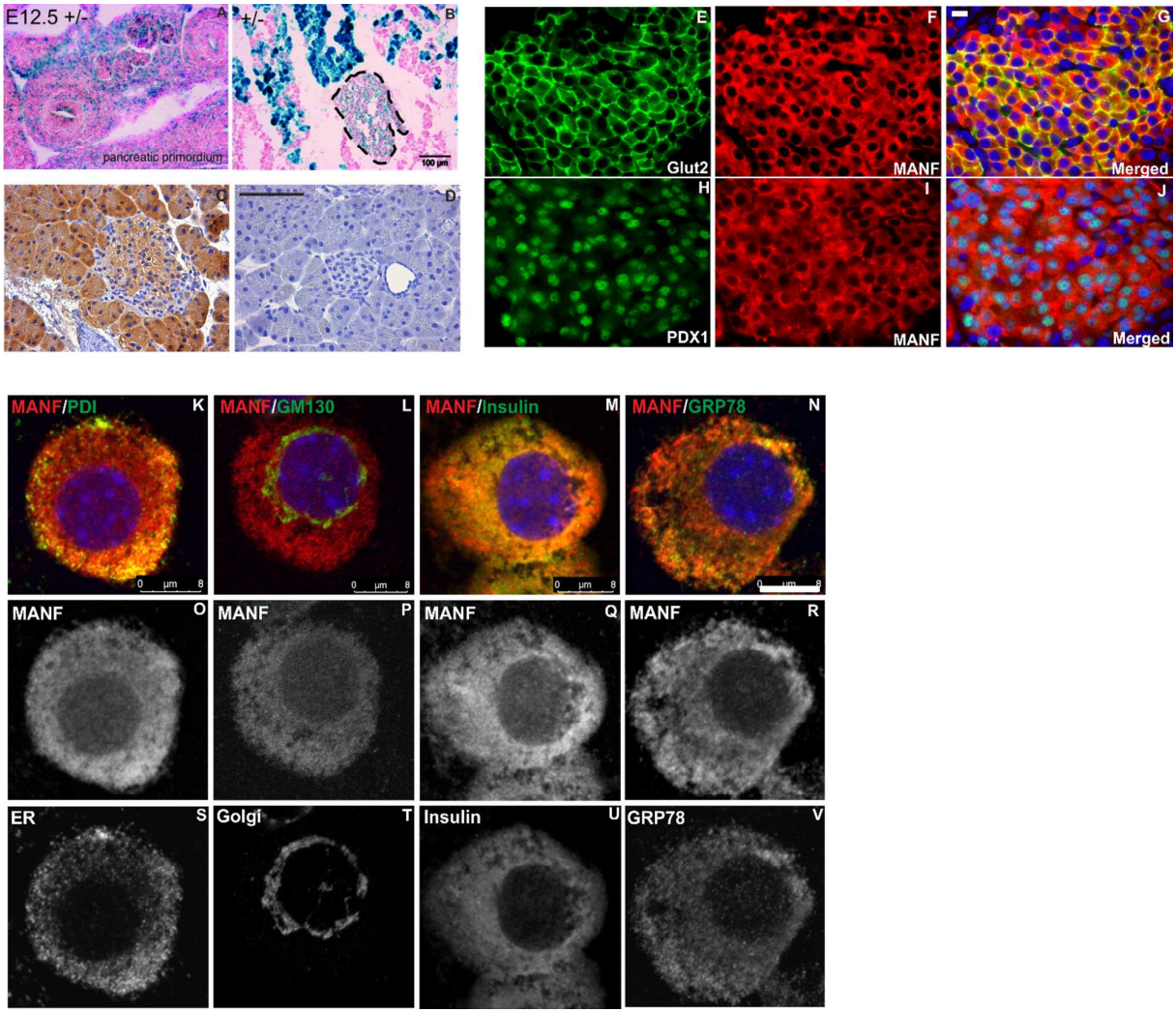

Supplementary Figure 1.1, supporting Figure 1. MANF is specifically expressed in the β-cell of the islets of Langerhans.

Detection of β-galactosidase activity under the control of MANF promoter in E12.5 pancreatic primordium and adult pancreas was detected by X-gal staining in *Manf*$^{+/-}$ heterozygote chimeric animals. **(A, B)** LacZ stained (blue) cryosections counterstained with nuclear fast red (pink) from *Manf* $^{+/-}$ chimeric embryo at E12.5 **(A)** and from adult *Manf* $^{+/-}$ chimeric pancreas **(B)**. Scale bar, 100 µm.

(C-D) Immunohistochemical localization of MANF protein in *Manf* $^{+/+}$ **(C)** and in *Manf* $^{-/-}$ **(D)** pancreas as negative control by using anti-ARP (MANF) antibody (Santa Cruz). Scale bar, 100 µm.

(E-J) Double immunohistochemistry analysis with MANF **(F, I)** GLUT2 **(E)**, and PDX1 **(H)**. Nearly all MANF positive cells (red) expressed GLUT 2 at the cell membrane of β-cells **(E-G)** whereas all MANF-positive cells showed nuclear staining for PDX1 (green) **(H-J)**. Cell nuclei were labelled with DAPI (blue). Scale bar, 10 µm.

(K-V) Representative confocal laser scanning microscopy images of double immunocytochemistry analysis of primary mouse β-cells using anti-MANF antibody (red) **(K-R)** with anti-PDI (Protein Disulphide Isomerase, ER marker, green) **(K, S)**, anti-GM130 (Golgi marker, green) **(L, T)**, anti-insulin (green) **(M, U)** and anti-GRP78 (green) **(N, V)** antibodies. Scale bar, 8 µm.

Supplementary Figure 1.2

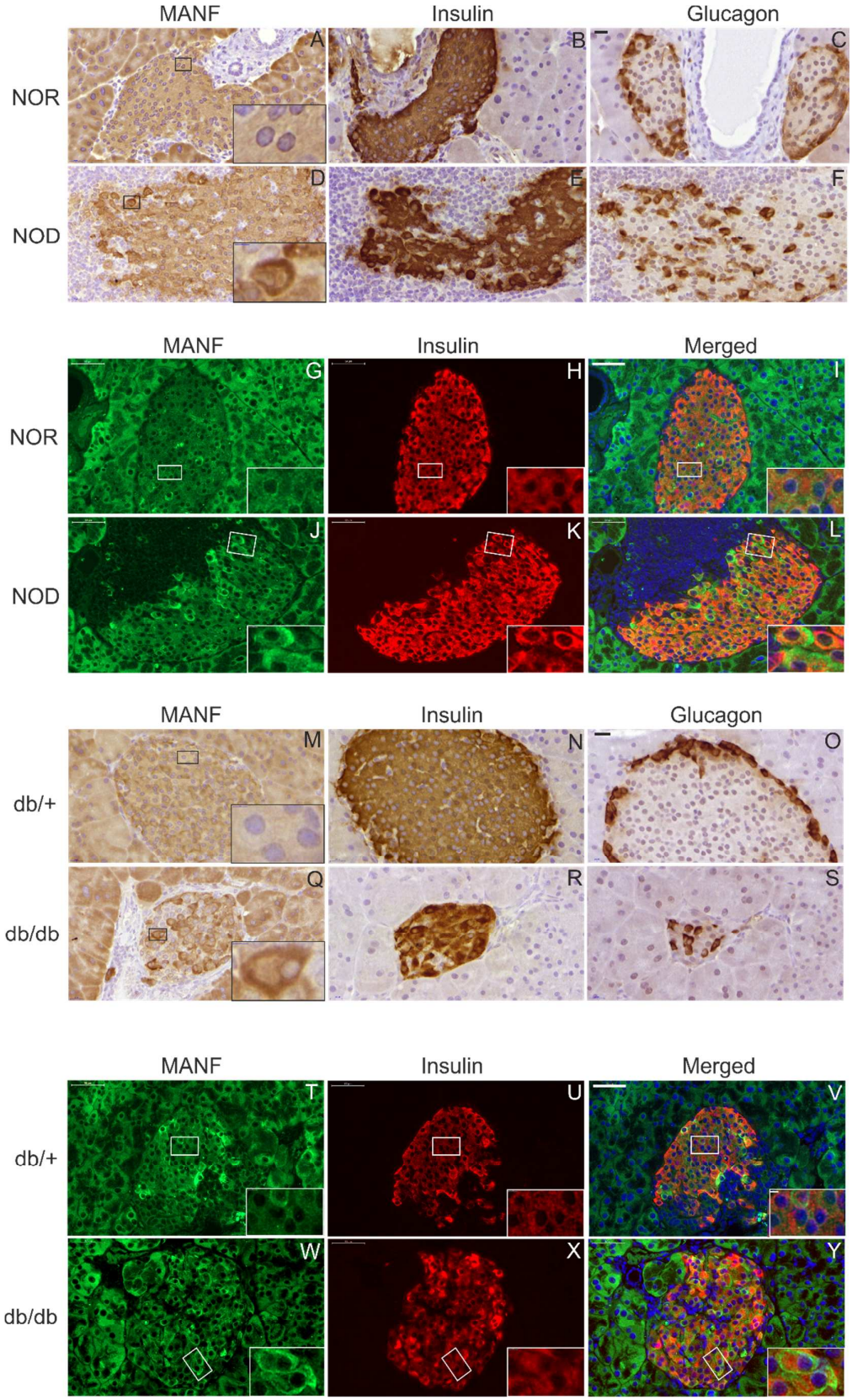

Supplementary Figure 1.2, supporting Figure 1. MANF expression in the β-cells of diabetic mouse models NOD and db/db.

(A-F) MANF **(A, D),** insulin **(B, E)** and glucagon **(C, F)** immunohistochemistry on pancreas sections from 11-week-old NOR (A, B, C) and NOD (D, E, F) mice. Scale bar, 20 µm.

(G-L) Double immunohistochemistry on pancreatic sections from 11-week-old NOR and NOD mice with anti-MANF (green) **(G, J)** and anti-insulin antibodies (red) **(H, K)** show increased MANF expression in β-cells in the periphery of islets near lymphocytic inflammatory cells invading the islets. Cell nuclei in merged pictures **(I, L)** labelled with DAPI (blue). Scale bar, 50µm.

(M-S) MANF **(M, Q),** insulin **(N, R)** and glucagon **(O, S)** immunohistochemistry on pancreas sections from 8-week-old db/+ **(M, N, O)** and db/db **(Q, R, S)** mice. Scale bar, 20 µm.

(T-Y) Double immunohistochemistry with anti-MANF (green) **(T, W)** and anti-insulin antibodies (red) **(U, X)** revealed disturbed islet architecture (W, X) and increased expression of MANF in some db/db islet β-cells (X) whereas others appeared to have reduced expression compared to MANF-stained β-cells in the control db/+ islets in 8-week-old mice. Cell nuclei in merged picture **(V, Y)** labelled with DAPI (blue). Scale bar, 50µm.

Supplementary Figure 2.1

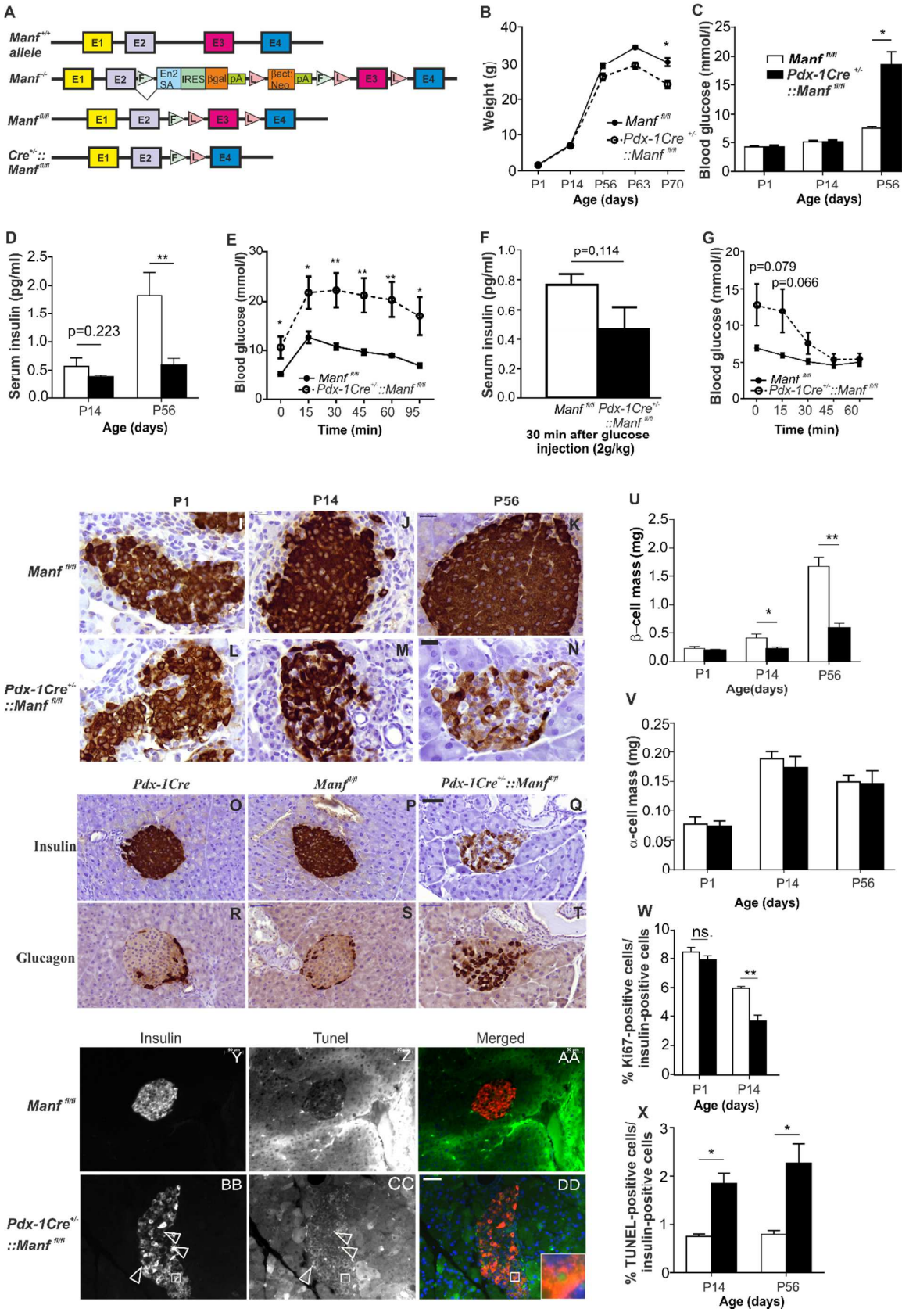

Supplementary Figure 2.1, supporting Figure 2. Absence of MANF in pancreas results in diabetes in *Pdx-1Cre*$^{+/-}$::*Manf*$^{fl/fl}$ mice.

(A) Schematic representation of the *Manf*$^{+/+}$wild-type, *Manf*$^{-/-}$, *Manf*$^{flox/flox(fl/fl)}$ and *Cre*::*Manf* $^{fl/fl}$ targeted allele. The strong splice-acceptor and β-galactosidase cassette was removed by crossing of *Manf* $^{+/-}$ to *CAG-Flp* transgenic mice in order to produce *Manf*$^{fl/fl}$ mice, where exon 3 is flanked with LoxP sites enabling removal in Cre-expressing cells. β-galactosidase reporter cassette (β-gal), strong splicing acceptor site (En2SA), exon (E), Frt (F)-sites, LoxP (L)-sites, βAct::Neo; human β-actin promoter driven neomycin resistance gene.

(B) Growth curve of *Manf*$^{fl/fl}$ and *Pdx-1Cre*$^{+/-}$::*Manf*$^{fl/fl}$ littermates. P1–P56, *n* =5-18 per group, combined from both sexes.

(C) Ad libitum-fed blood glucose levels, *n*=9-21 per group;

(D) Serum insulin levels from ad libitum-fed mice, *n* = 9–15 per group;

(E) Blood glucose levels measured after intraperitoneal glucose (2 g/kg) injection, *n* =8-9 mice per group.

(F) Serum insulin levels in P56 mice measured 30 min after glucose (2 g/kg) bolus injection, *n* =7 mice per group.

(G) Blood glucose levels measured after intraperitoneal injection of insulin (1 U/kg), *n* =7-8 mice per group.

(I-N) Insulin immunohistochemistry on pancreas sections from *Manf*$^{fl/fl}$ **(I-K)** and *Pdx-1Cre*$^{+/-}$::*Manf*$^{fl/fl}$ **(L-N)** animals at P1 **(I, L)**, P14 **(J, M)**, and P56 **(K, N)**. The scale bar represents 20 μm.

(O-T) Insulin **(O-Q)** and glucagon **(R-T)** immunohistochemistry on pancreas sections from P56 *Pdx-1Cre, Manf*$^{fl/fl}$ and *Pdx-1Cre*$^{+/-}$::*Manf*$^{fl/fl}$ mice. Scale bar, 50 μm.

(U) Reducedβ-cell mass in *Pdx-1Cre*$^{+/-}$::*Manf*$^{fl/fl}$ mice from P14, *n* = 6-20 per group.

(V) α-cell mass in *Pdx-1Cre*$^{+/-}$::*Manf*$^{fl/fl}$ mice, *n* = 5-7 per group.

(W) β-cell proliferation assessed by Ki67 and insulin staining, *n* =5-12 per group.

(X) β-cell apoptosis assessed by TUNEL and insulin staining, *n* =5-12 per group.

(Y-DD) Double immunohistochemistry on pancreas sections from *Manf*$^{fl/fl}$ and *Pdx-1Cre*$^{+/-}$::*Manf*$^{fl/fl}$ pancreases at P56 using TUNEL (green)- and anti-insulin (red) staining. Arrowheads point to TUNEL-positive β-cell (R). Scale bar 50 μm.

Values represent mean ± SEM, *p < 0.05, **p < 0.01, ***p< 0.001.

Supplementary Figure 2.2

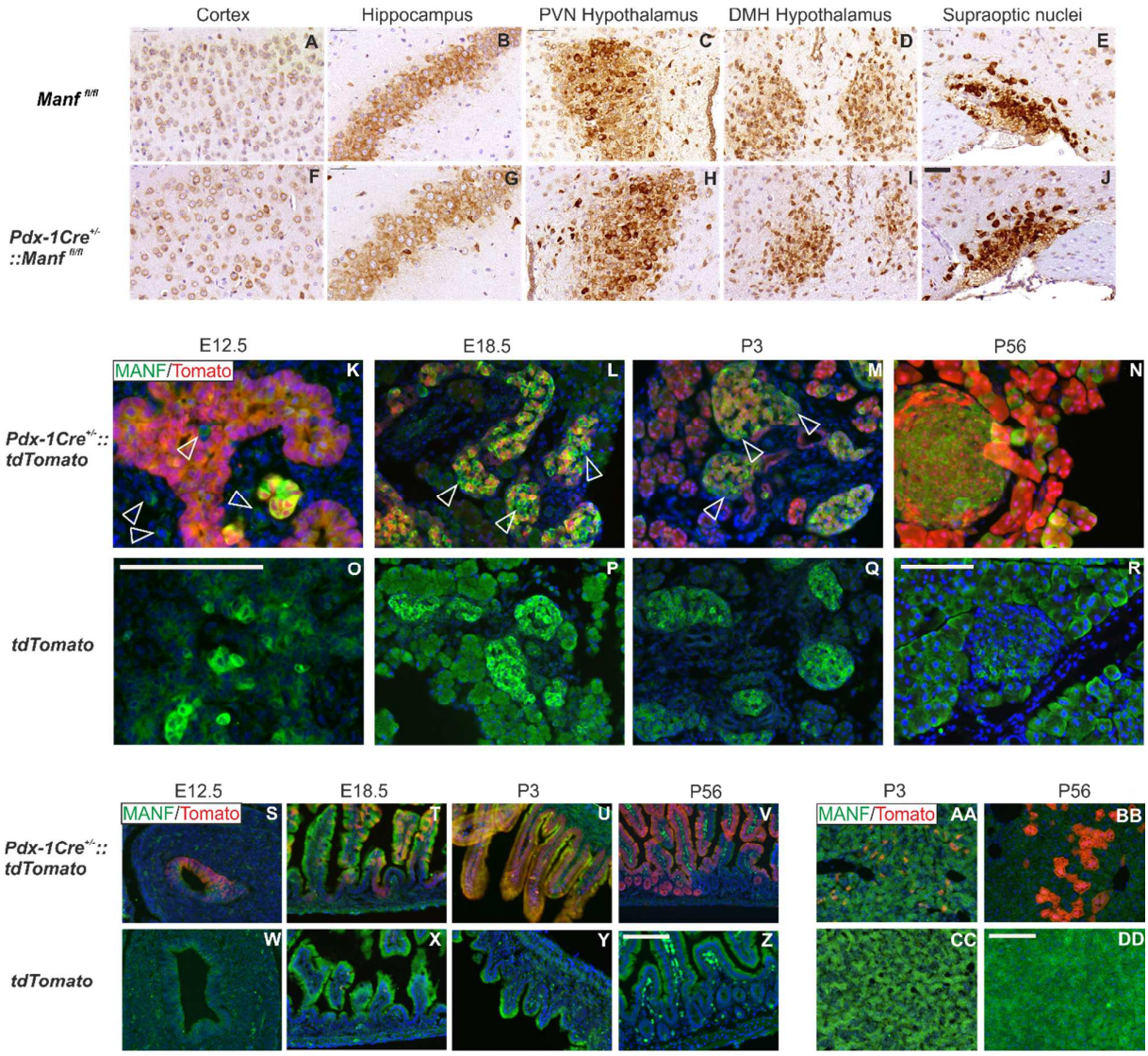

Supplementary Figure 2.2, supporting Figure 2. Analysis of Pdx-1 Cre recombinase activity

(A-J) MANF immunohistochemistry on brain sections from *Manf*$^{fl/fl}$ **(A-E)** and *Pdx-1Cre*$^{+/-}$ ::*Manf*$^{fl/fl}$ mice **(F-J)**. No visible differences were observed in MANF expression in the cortex **(A, F)**, hippocampus **(B, G)**, paraventricular nuclei of hypothalamus (PVN) **(C, H)**, dorsal medial nuclei of hypothalamus (DMH) **(D-I)** and supraoptic nuclei of hypothalamus **(E, J)**. Scale bar, 50µm.

(K-R) Co-expression of MANF and tdTomato red fluorescent protein. Double immunohistochemistry analysis of MANF (green) and tdTomato (red) expression in the pancreases of *Pdx-1Cre*$^{+/-}$::*tdTomato* **(K-N)** and *tdTomato* mice **(O-R)**. dtTomato expression was observed in developing pancreatic primordium at E12.5, when high MANF signal was detected in some cells of the pancreatic primordium probably representing insulin-positive cells **(K)**. At E18.5 **(L)** Tomato expression was detected in the islet nuclei of MANF positive cell. At P3 **(M)** and P56 **(N)** Tomato expression was found in the nuclei of endocrine islets and in exocrine tissue mostly overlapping with MANF expression. However, some MANF-positive cells lacked Tomato expression, explaining the incomplete deletion of MANF from pancreas tissue leading to mosaic expression of MANF in *Pdx-1Cre*$^{+/-}$::*Manf*$^{fl/fl}$ mice. Notably, no Tomato signal was observed in the *tdTomato* mice lacking Cre, indicating that the system is not leaky **(O-R)**. Cell nuclei were labelled with DAPI (blue). Scale bar, 100 µm.

(J-Q) Merged pictures of double immunohistochemistry analysis with MANF and Tomato expression in the duodenum region of the intestine of *Pdx-1Cre*$^{+/-}$::*tdTomato* **(S-V)** and *tdTomato* mice **(W-Z)**. MANF and Tomato expression was observed in developing intestine at E12.5 **(S)**. At E18.5 **(T)**, P3 **(U)**, P56 **(V)** Tomato expression was detected in the villi of duodenum with mosaic expression pattern. Notably, no positive Tomato signal was observed in the *tdTomato* mice, indicating the specificity of the expression pattern in *Pdx-1Cre*$^{+/-}$::*tdTomato* **(W-Z)**. Cell nuclei were labelled with DAPI (blue). Scale bar, 100 µm.

(AA-DD) Merged pictures of double immunohistochemistry analysis with MANF and Tomato expression in the liver of *Pdx-1Cre*$^{+/-}$::*tdTomato* **(AA, BB)** and *tdTomato* mice **(CC, DD)**. Surprisingly, few positive Tomato cell were detected in the liver of P3 **(AA)** and P56 **(BB)** in *Pdx-1Cre*$^{+/-}$::*tdTomato.* However, no positive Tomato expression was observed in E18.5 **(R, U).** Notably, no positive Tomato signal was observed in the *tdTomato* mice, indicating the specificity of the expression pattern in *Pdx-1Cre*$^{+/-}$::*tdTomato* **(CC, DD)**. Cell nuclei were labelled with DAPI (blue). Scale bar, 100 µm.

Supplementary Figure 2.3

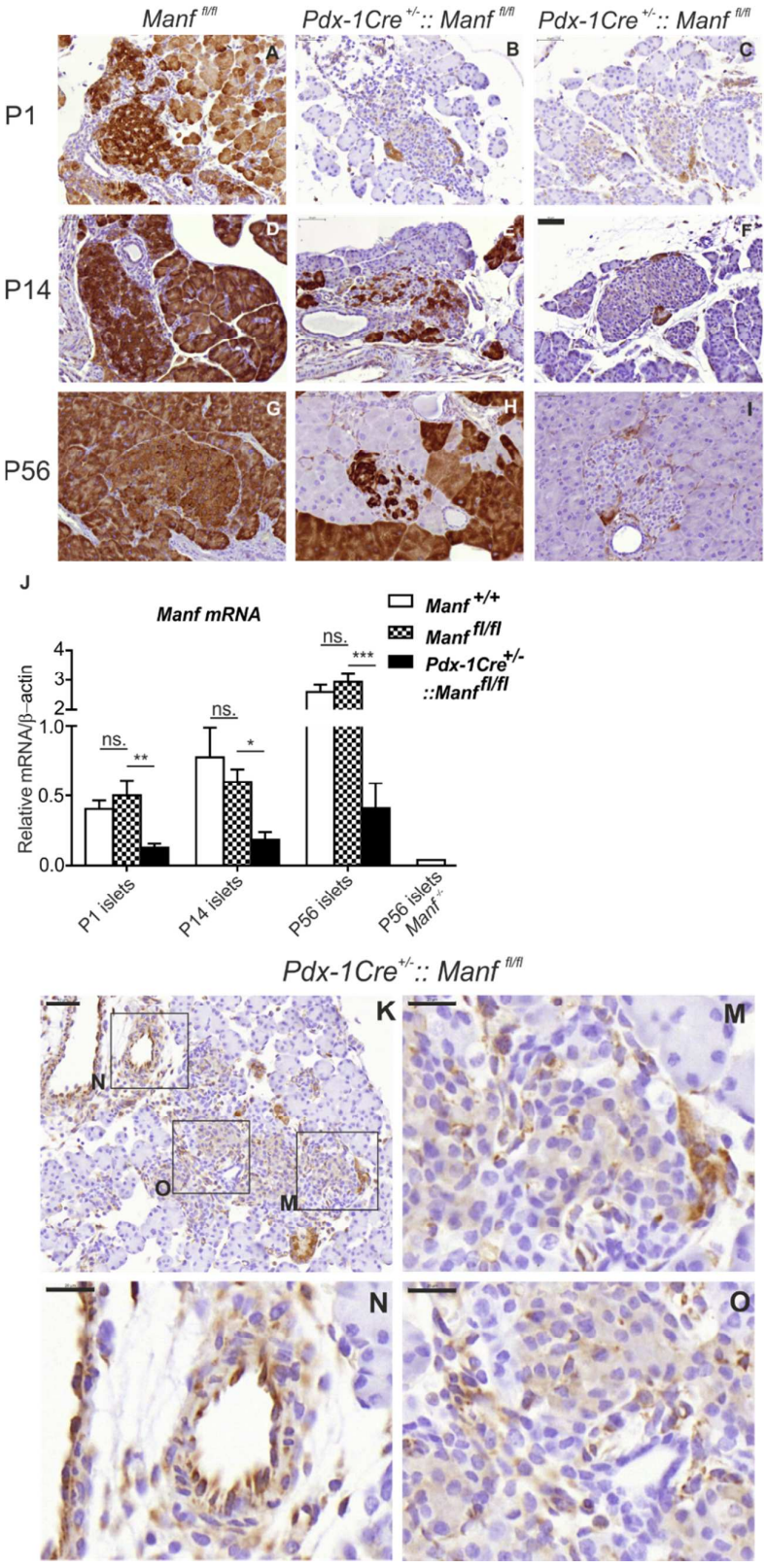

Supplementary Figure 2.3, supporting Figure 2. MANF expression level in the pancreases of *Pdx-1Cre$^{+/-}$::Manf$^{fl/fl}$* mice is highly variable between individual mice

(A-I) Immunohistochemical peroxidase staining of MANF protein in *Manf*$^{fl/fl}$ **(A, D, C)** and *Pdx-1Cre*$^{+/-}$::*Manf*$^{fl/fl}$ **(B-C, E-F, H-I)** mice at P1 **(A-C)**, P14 **(D-F)**, and P56 **(G-I)**. Scale bar, 50 μm.

(J) Quantitative RT-PCR analysis for *Manf* mRNA levels in pancreatic islets isolated from *Manf*$^{+/+}$, *Manf*$^{fl/fl}$ and *Pdx-1Cre*$^{+/-}$::*Manf*$^{fl/fl}$ mice at P1 (n=6) , P14 (n=9) and P56 (n=10). *Manf* mRNA levels were significantly decreased in the islets of *Pdx-1Cre*$^{+/-}$::*Manf*$^{fl/fl}$ compared to *Manf*$^{fl/fl}$ islets. No difference in *Manf* mRNA expression levels was observed between *Manf*$^{fl/fl}$ and *Manf* $^{+/+}$ islets confirming that the remaining Frt-site and LoxP sites in the introns flanking exon 3 in the *Manf*$^{fl/fl}$ gene does not disturb correct MANF pre-mRNA splicing and mRNA expression. Values represent mean ± SEM. *$p < 0.05$, **$p < 0.01$, ***$p< 0.001$.

(K-N) Immunoperoxidase staining of MANF protein in P1 *Pdx-1Cre*$^{+/-}$::*Manf*$^{fl/fl}$ pancreas sections. MANF positive cells observed within the Langerhans islets **(L, N),** ducts and blood vessels **(M)** in the P1 pancreas of *Pdx-1Cre*$^{+/-}$::*Manf*$^{fl/fl}$ mice. Scale bar, 50 μm, **(L-N)** Scale bar, 20 μm.

Supplementary Figure 3

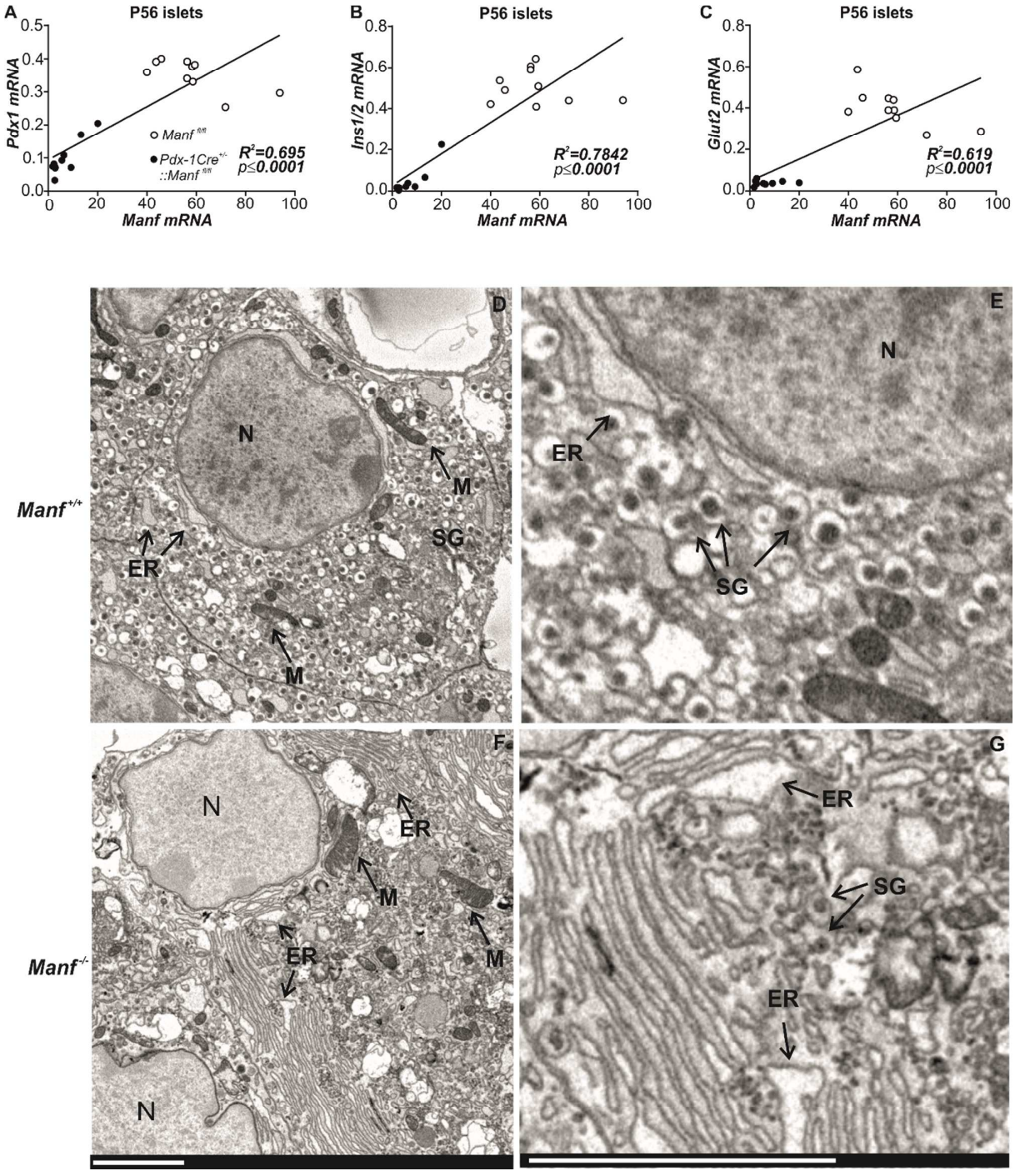

Supplementary Figure 3, supporting Figure 3. Positive correlation of *Manf* mRNA with mRNA levels of β-cell specific genes and ultrastructural morphology of islet β-cells in 4-week-old *Manf*$^{-/-}$ pancreas.

(A-C) Positive correlation of *Manf* mRNA with *Pdx-1* **(A)**, *Ins1/2* **(B)**, *Glut2* **(C)** mRNAs was observed between P56 *Pdx-1Cre*$^{+/-}$::*Manf*$^{fl/fl}$ and *Manf*$^{fl/fl}$ mice. *n* =9-10 mice per group.

(D-G) Representative electron microscopy images of islets from 4-week-old *Manf*$^{+/+}$ **(D, E)** and *Manf*$^{-/-}$ **(F, G)** mice. Nucleus (N), endoplasmic reticulum(ER), secretory granule (SG), mitochondria (M). The loss of insulin secretory granules, enlarged mitochondria and dilated ER indicates ER stress-induced forthcoming β-cell demise in *Manf*$^{-/-}$ β-cells. Scale bar, 3 μm.

Supplementary Figure 4

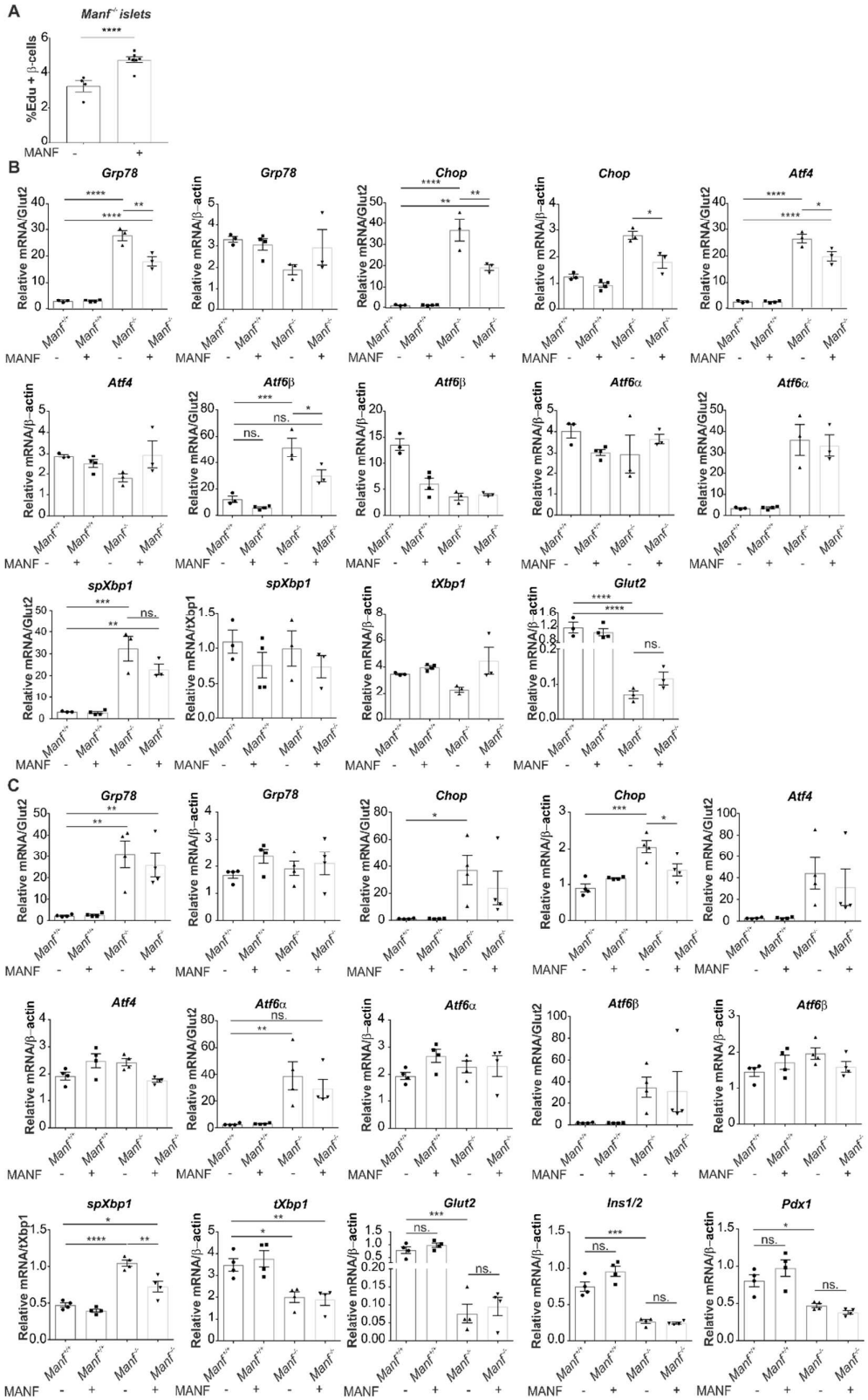

Supplementary Figure 4, supporting Figure 4. MANF induces proliferation of *Manf*$^{-/-}$ β-cells and reduces ER stress caused by MANF-deficiency in β-cells.

(A) Recombinant MANF protein at a concentration of 100 ng/ml increases proliferation of β-cells from 4-5-week-old *Manf*$^{-/-}$ mice after 5 days in culture. *n* =quantified from 4-7 wells per group.

(B) Quantitative RT-PCR PCR analysis of UPR genes *Atf4*, *Grp78*, *Chop*, *spXbp1, tXbp*, *Atf6a*, *Atf6β* and of β-cell marker *Glut2* from the isolated islets from 4-week-old *Manf*$^{+/+}$ and *Manf*$^{-/-}$ mice treated with 1 μg/ml human recombinant MANF overnight in 0.5% BSA medium. Human recombinant MANF is able to reduce ER stress in *Manf*$^{-/-}$ islets by downregulating UPR markers. *n* = 3-4 per group.

(C) Quantitative RT-PCR PCR analysis of UPR genes *Atf4*, *Grp78*, *Chop*, *spXbp1, tXbp*, *Atf6a*, *Atf6β* and of β-cell markers *Glut2, Pdx1 and Ins1/2* from isolated islets of 4-week-old *Manf*$^{+/+}$ and *Manf*$^{-/-}$ mice treated with 100 ng/ml human recombinant MANF for 3 days in 10% FBS medium. Human recombinant MANF is able to reduce expression levels of UPR markers *Chop* and *spXbp1* mRNA in isolated islets of *Manf*$^{-/-}$ mice. Additionally, a small but insignificant increase was detected in *Ins1/2* and *Pdx1* mRNA expression in *Manf*$^{+/+}$ islets treated with MANF for 3 days. *n* = 3-4 per group.

Values represent mean ± SEM. *$p < 0.05$, **$p < 0.01$, ***$p< 0.001$, ****$p< 0.0001$.

Supplementary Figure 5.1

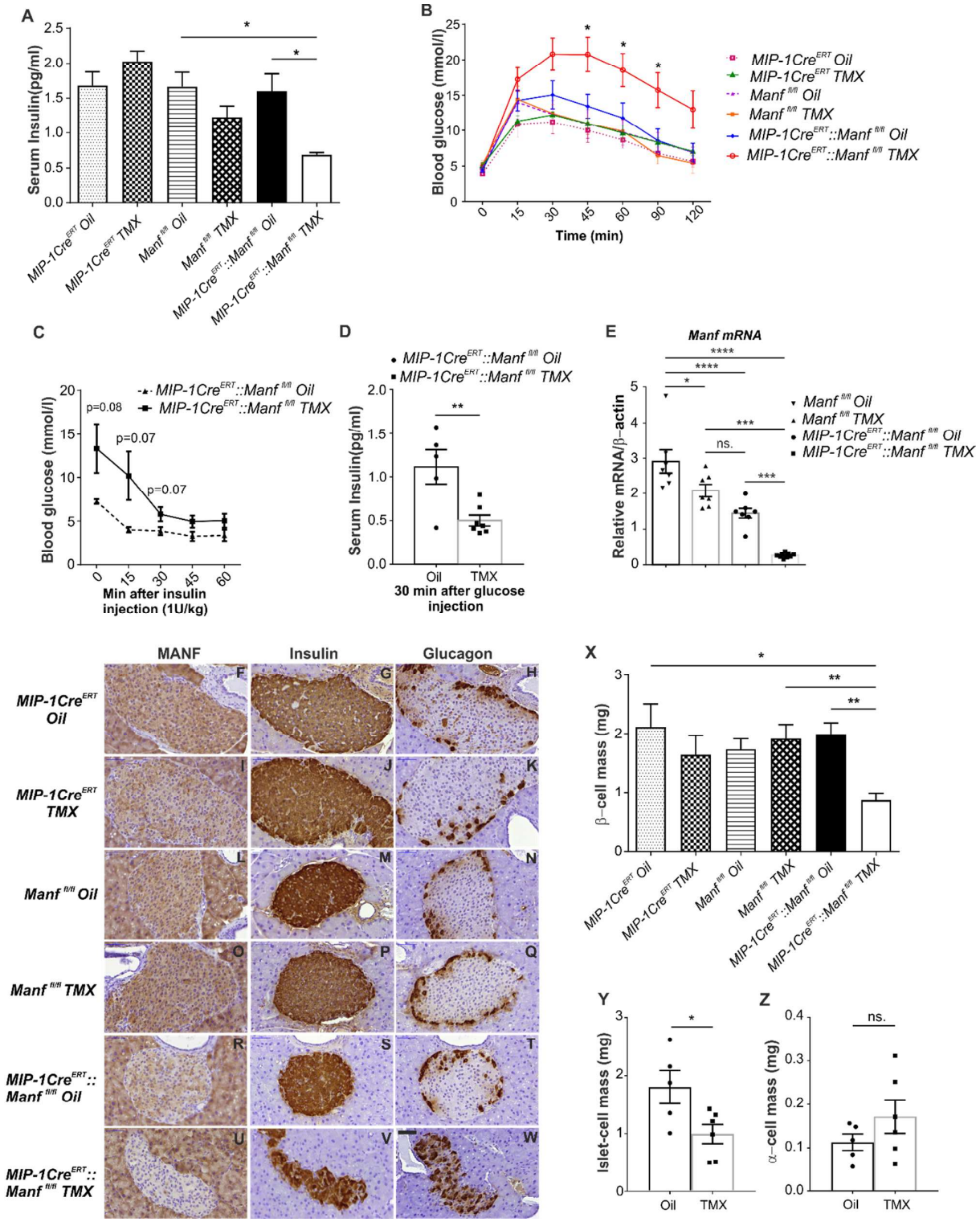

Supplementary Figure 5.1, supporting Figure 5. MANF-deletion in adult β-cells results in reduced β-cell mass and diabetes *in vivo* in *MIP-1Cre^{ERT}::Manf$^{fl/fl}$* mice.

(A) Serum insulin levels measured 4 weeks after tamoxifen or oil injection from *ad libitum*-fed mice, *n* = 2-13 mice per group.
(B) Blood glucose levels measured after intraperitoneal glucose (2 g/kg) injection, *n* =2-12 mice per group.

(C) Blood glucose levels measured after intraperitoneal insulin injection (1 U/kg), *n* = 4-6 mice per group.

(D) Serum insulin levels measured from P90 mice 30 min after glucose bolus injection (2 g/kg), *n* =5-7 mice per group.

(E) Relative *Manf mRNA* levels in islets isolated from *Manf $^{fl/fl}$* mice injected with oil or tamoxifen and in islets from *MIP-1Cre^{ERT}::Manf$^{fl/fl}$* injected with oil or tamoxifen. *n* = islets from 7-9 mice per group.

(F-W) Immunohistochemical analysis of MANF **(F, I, L, O, R, U),** insulin **(G, J, M, P, S, V)** and glucagon-positive **(H, K, N ,Q ,T ,W)** cells in pancreatic sections reveals morphological changes in the islets of from *MIP-1Cre^{ERT}::Manf$^{fl/fl}$* injected with tamoxifen compared to control mice. Scale bar, 50 µm.

(X) The β-cell mass is significantly reduced in P90 *MIP-1Cre^{ERT}::Manf$^{fl/fl}$* mice injected with Tmx, compared to the β-cells mass in control mice, *n* = 2-6 mice per group.

(Y) The islet**-**cell mass quantified from Chromogranin A antibody-stained sections is significantly reduced in adult *MIP-1Cre^{ERT}::Manf$^{fl/fl}$* mice injected with TMX, compared to the islet-cell mass in control *MIP-1Cre^{ERT}::Manf$^{fl/fl}$* mice injected with oil, *n* = 5-6 mice per group.

(Z) α-cell mass in in P90 *MIP-1Cre^{ERT}::Manf$^{fl/fl}$* mice injected with Tmx, compared to the α-cell mass in control *MIP-1Cre^{ERT}::Manf$^{fl/fl}$* mice injected with oil , *n* = 5-6 mice per group.

Mean ± SEM, *p < 0.05, **p < 0.01, ***p< 0.001, ****p< 0.0001 versus the corresponding control.

Supplementary Figure 5.2

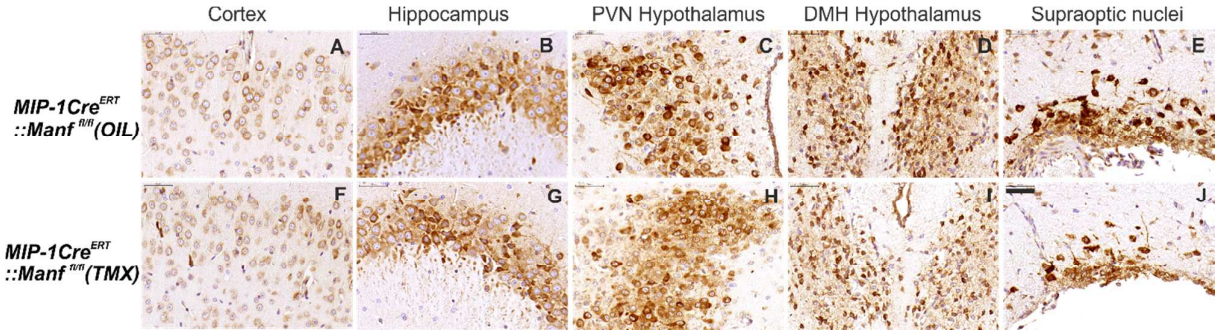

Supplementary Figure 5.2, supporting Figure 5. MANF expression in the brain of *MIP-1Cre^{ERT}::Manf$^{fl/fl}$ mice*.

(A-J) Immunohistochemistry of MANF protein in brain sections from P90 oil-injected *MIP-1Cre^{ERT}::Manf$^{fl/fl}$(OIL)* **(A-E)** and tamoxifen-injected *MIP-1Cre^{ERT}::Manf$^{fl/fl}$(TMX)* **(F-J)**. No noticeable changes were detected in MANF expression in the cortex **(A, F)**, hippocampus **(B, G)**, paraventricular nuclei of hypothalamus (PVN) **(C, H)**, dorsal medial nuclei of hypothalamus (DMH) **(D-I)** and supraoptic nuclei of hypothalamus **(E, J)** between the different genotypes. Scale bar, 50µm.

Supplementary Figure 6

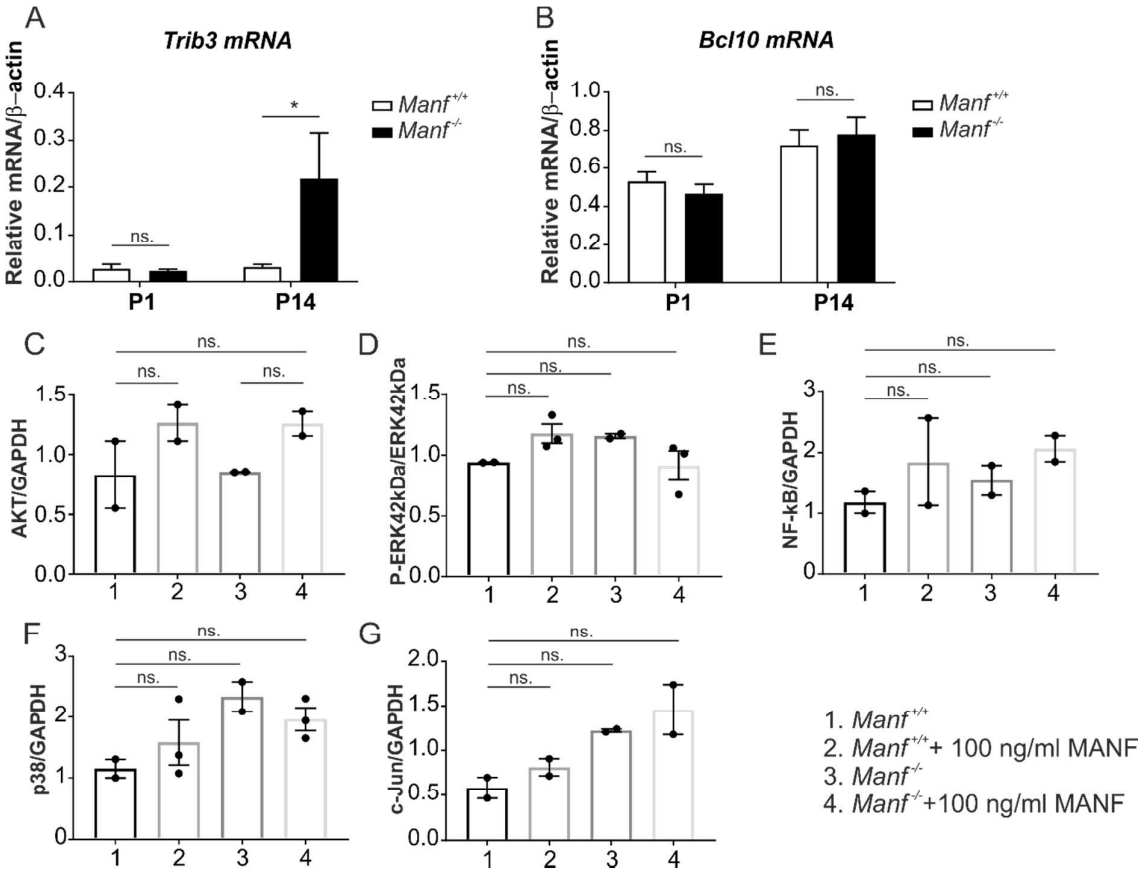

Supplementary Figure 6, supporting Figure 7. Insights in the MANF mechanism of action

(A-B) Relative *Trib3* and *Bcl10 mRNA* levels in islets isolated from *Manf*$^{+/+}$ and *Manf*$^{-/-}$ mice at postnatal day 1 (P1) and P14. *n* = islets from 3-5 mice per group.

(C-G) Quantitative analysis of the western blot bands normalized to either total protein or GAPDH, 1. *Manf*$^{+/+}$ islets, 2. *Manf*$^{+/+}$ islets cultured in the presence of 100 ng/ml of human recombinant MANF, 3. *Manf*$^{-/-}$ islets, 4. *Manf*$^{-/-}$ islets cultured in the presence of 100 ng/ml of human recombinant MANF. Mean ± SEM, *p < 0.05, ns., non-significant, of two independent experiments. *n* = 2-3.

Supplementary Table 1. Primary antibodies used in the study

Peptide/Protein target	Catolog number, Manufacture	Species raised in	Dilution	Country of origin
MANF	310-100, Icosagen	rabbit polyclonal	1:1000	Tartumaa, Estonia
MANF(ARP) C-19	sc-34560, Santa Cruz Biotechnology	goat polyclonal	1:500	Texas, USA
Insulin	ab7842, Abcam	guinea pig polyclonal	1:200	guinea pig polyclonal
Insulin	A0564, Dako	guinea pig polyclonal	1:2000	Santa Clara, California, US
Glucagon	ab10988, Abcam	mouse monoclonal	1:1000	Cambridge, UK
PDX1	07-696, Millipore	rabbit polyclonal	1:500	Billerica, Massachusetts, US
GLUT2	C-19, sc-7580, Santa Cruz Biotechnology	goat polyclonal	1:1000	Texas, USA
PP	A0619, Dako	rabbit polyclonal	1:600	Santa Clara, California, US
Somatostatin	A0566, Dako	rabbit polyclonal	1:200	Santa Clara, California, US
Ki67 (Clone SP6)	RM-9106, ThermoFisher Scientific	rabbit monoclonal	1:150	Waltham MA, USA
PDI	ADI-SPP-891-F, Enzo/AH Diagnostics	mouse monoclonal	1:200	Farmingdale, NY, USA
GM130	610823, BD Transduction Laboratories	mouse monoclonal	1:200	San Jose, CA, USA
GRP78(C-20)	sc-1051, Santa Cruz Biotechnology	goat polyclonal	1:500	Texas, USA
GAPDH	MAB374, Millipore	mouse monoclonal	1:3000	Billerica, Massachusetts, US
P-Akt	4058, Cell Signaling Technology	rabbit monoclonal	1:100	Danvers, MA, US
Akt	40D4,2920, Cell Signaling Technology	mouse monoclonal	1:500	Danvers, MA, US
P-p38	4631, Cell Signaling Technology	rabbit monoclonal	1:100	Danvers, MA, US

p-38	9218, Cell Signaling Technology	rabbit polyclonal	1:500	Danvers, MA, US
P-ERK1/2	E-4, sc-7383, Santa Cruz Biotechnology	mouse monoclonal	1:100	Texas, USA
ERK1/2	K-23, sc-153 Santa Cruz Biotechnology	rabbit polyclonal	1:500	Texas, USA
P-c-Jun	Ser63, 2361, Cell Signaling Technology	rabbit monoclonal	1:500	Danvers, MA, US
c-Jun	9165, Cell Signaling Technology	rabbit monoclonal	1:500	Danvers, MA, US

Supplementary Table 1 continuation. Primary antibodies used in the study

Peptide/Protein target	**Catolog number, Manufacture**	**Species raised in**	**Dilution**	**Country of origin**
P-NF-κB	3033, Cell Signaling Technology	rabbit monoclonal	1:1000	Danvers, MA, US
NF-κB	8242, Cell Signaling Technology	rabbit monoclonal	1:1000	Danvers, MA, US
iNOS	M19, sc-650, Santa Cruz Biotechnology	rabbit polyclonal	1:500	Texas, USA
Chromogranin A	ab15160, Abcam	rabbit polyclonal	1:500	Cambridge, UK

Supplementary Table 2. Pearson´s correlation coefficient and Manders' coefficients for channel specific colocalization.

Slide name		Number of analysed cells	Pearson's coefficient Mean	Pearson's coefficient, Stderr	Mander's coefficient Mean	Mander's coefficient, Stderr
1	MANF	66	0.554	0.024	0.883	0.006
	ER				0.760	0.010
2	MANF	20	0.005	0.028	0.211	0.04
	Golgi				0.229	0.035
3	MANF	51	0.591	0.031	0.855	0.029
	Insulin				0.845	0.03
4	MANF	61	0.374	0.032	0.640	0.029
	GRP78				0.464	0.029